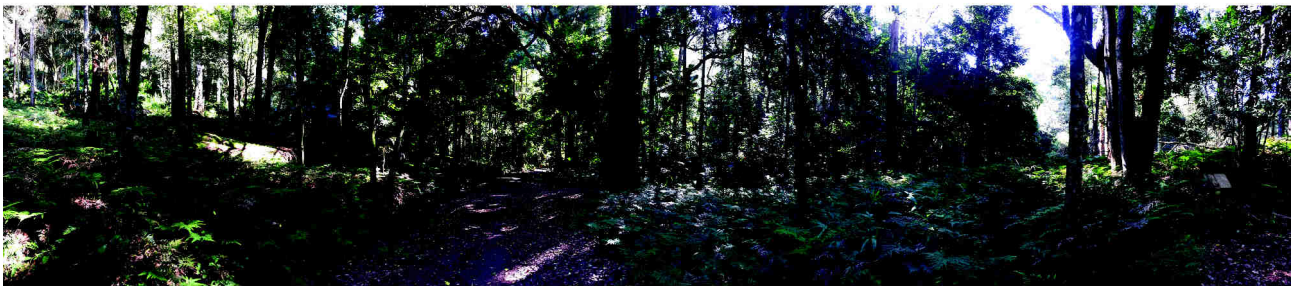# Remote Sensing of Wildland Bushfire Fuels in the Royal National Park, NSW

Royal National Park, NSW Australia. April 2016

Liam Turner, BSc/BEd MSc
Department of Environmental Sciences
Faculty of Science & Engineering
Macquarie University
Submission Date 10 October 2016

MACQUARIE
University
SYDNEY·AUSTRALIA

Declaration

I hereby declare that this thesis has not been previously submitted to any other institution or university for a higher degree. Except where otherwise acknowledged, this thesis is comprised entirely of my own work.

Signature

Liam Turner

10th October 2016

This thesis has been formatted to ensure compliance with a page limit of 50 pages for text and figures, determined by the Faculty of Science and Engineering at Macquarie University.

Acknowledgements

Abstract

Field based techniques assessing wildland bushfire fuel characteristics are limited by the spatial extent at which they can be implemented due to cost, labour intensity, and terrain accessibility. Within Australia, research using remote sensing instruments to assess fuel characteristics has utilised low resolution imagery, simultaneously assessing all fuel strata. Within this research, fuel load is used to quantify wildland fuel distribution. Fuel load has been suggested to not account for fuel particle arrangement. This thesis presents two manuscripts: the first investigates the fuel hazard classification of pan-sharpened imagery to improve bushfire fuel assessment resolution, and the second investigates machine learning algorithms and the fusion of LiDAR and high resolution imagery to classify a single fuel stratum, the understory. Results suggest that the use of pan-sharpening to improve bushfire fuel assessment resolution is plausible, and that understory fuels can be classified with moderate accuracy using Support Vector Machine classification of a fusion of imagery and LiDAR metrics.

Contents

Chapter 1 Introduction

1.1   Background

### 1.1.1 Wildland Fire in Australia

In Australia, wildland fires, those which occur on uncultivated or uncleared land such as national parks and commonly referred to as bushfires, are an intrinsic part of the environment and a significant natural hazard[1]. Bushfires are not simply a physiochemical process, but rather a fundamental biogeochemical process occurring in the natural environment (Williams et al., 2012; Bowman et al., 2009). Native vegetation has evolved a range of strategies for surviving and reproducing after a fire, including loosely attached bark and leaves containing highly flammable oils which act as a catalyst to promote fire events (Cash, 2012; Keith, 2004). Fire also links biomass and the atmosphere through the release of gases from combustion, and nutrients into soils through decomposition (Williams et al., 2012). Successive fires can result in loss of habitat, changes to biodiversity levels, erosion, water quality effects and carbon emissions (Whelan et al., 2006). When proximal to urban areas or anthropogenic landscape features they pose a significant natural hazard causing the damage and destruction of property and loss of life (Middlemann, 2007).

1.1.2 Fuel and Fire Behaviour

Bushfire, although significant, is a natural hazard for which the potential impacts can be minimised before a fire occurs (Middlemann, 2007). This minimisation is undertaken through the management of fuels, which influence a fire's behaviour. Fire is described by a complex set of chain oxidation reactions (Cheney and Sullivan, 2008; Keane, 2015). At their finest scales these reactions require heat, oxygen, and fuel to occur (Countryman, 1969; Keane, 2015), often illustrated through the fire triangle (see Figure 1.1.1). In a wildland environment, oxygen is supplied by the atmosphere and fuel supplied by biomass, which is susceptible to burn because of it's organic chemical constituency (Keane, 2015). Heat or ignition, required to start the reaction, can come from both human and natural, means such as arson or lightning, respectively. Fuels are defined as live or dead biomass available for combustion, which influences the development and propagation of a fire through their arrangement, structure and chemical composition (Hollis et al., 2015; Williams et al., 2012; Keane, 2015). When this definition is applied across increasing spatial and temporal scales it is clear that knowledge of fuel characteristics which influence a fire are fundamental to making predictions about their behaviour, as illustrated in Figure 1.1.1.

---

[1]Within this thesis the terms bushfire and wildland fire are used interchangeably.
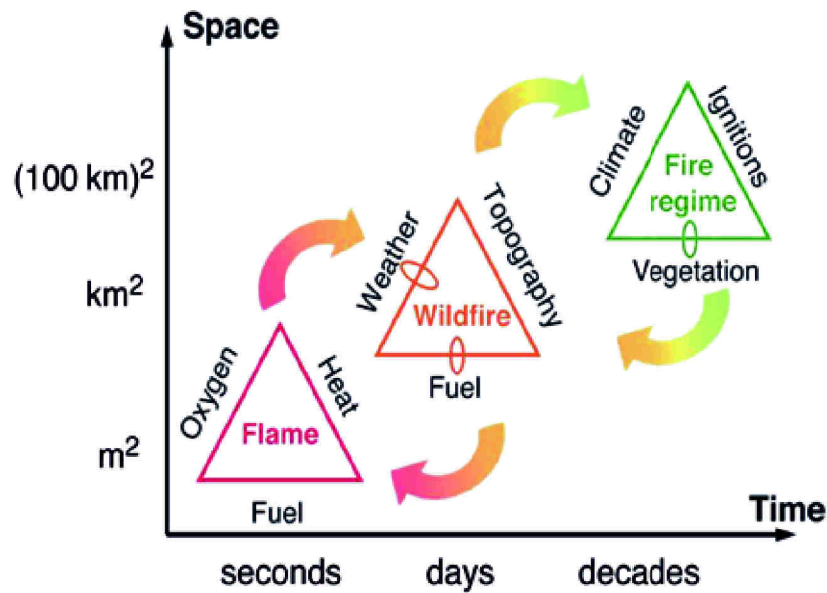
Figure 1.1.1: A plot of the fire triangle over spatial and temporal scales. The fire triangle describes the factors influencing fire behaviour, how they change across space and time (arrows), and the feedbacks fire has on them (loops). Source: Moritz et al. (2005).

In order to assess fuels for management purposes, models which link fuel characteristics to fire behaviour need to be defined. Traditionally, fire behaviour modelling research has followed a geographic, empirical vs mechanistic dichotomy (Cruz and Gould, 2009). In Australia, empirical models which statistically correlate experimental fire behaviour with input characteristics are used (Sullivan, 2009*a*). In North America, mechanistic or physical models, are formulated as expressions of the underlying theory of the physical processes at play (Sullivan, 2009*a*; Cruz and Gould, 2009). Due to the nature of technology the used to develop models, the outputs of fire behaviour models have historically been one dimensional quantifications such as forward rate of spread, or flame height. This is because the level of sophistication of the model tends to match that of the technology used to implement them. With the development of computer technology it is now possible to integrate both empirical and mechanistic fire behaviour models with propagation algorithms to simulate a fire's behaviour over a landscape (Sullivan, 2009*b*). These models, known as fire behaviour simulation models, have been developed in both North America and Australia for mechanistic (Finney and Andrews, 1999) and empirical (Tolhurst et al., 2008) fire behaviour models, respectively. It should be noted however, that attempts to apply North American fire behaviour models within Australia, and other models across jurisdictions have not been successful (Watson, 2009; Fogarty et al., 1998). Therefore for this study, only fuel characteristics pertaining to empirical and fire behaviour simulation models developed for Australia will be considered.

In Australia, research into modelling fire behaviour was pioneered in the late 1950s and early 1960s by A. G. McArthur in Eastern Australia and by G. B. Peet in Western Australia (Cruz and Gould, 2009). Their experiments consisted of igniting point source fires for various vegetation types such as forests and grasslands which were allowed to spread for varying times, while weather (e.g., wind speed, and air temperature) and fire behaviour characteristics (e.g., rate of spread) were monitored (Cruz and Gould, 2009). The models developed from these experiments were made available to users in a variety of forms such as numerical tables, and slide rules. These models take estimates of local weather conditions, fuel moisture, and structure as inputs and output quantified fire behaviour measurements such as rate of forward spread (Cruz et al., 2014). While moisture and weather conditions are significant factors influencing fire behaviour, this thesis limits its scope to the assessing the structure and spatial distribution of fuels.

Within fire behaviour modelling, unique fuel vegetation groups exhibit an identifiable association of fuel elements with a distinctive species, form, size, arrangement and continuity, which together, have characteristic fire behaviour under defined burning conditions (Merrill and Alexander, 1987). Since the 1950's, a number of other models have been developed for other fuel vegetation groups found within Australia (see Cruz et al. (2014)). From these experiments it was identified that different variables, some unique to each fuel group, influence fire behaviour in different ways.

1.1.3 Assessing Fuel Structure

Fuel structure, within and across different fuel vegetation groups, can be assessed and quantified in a number of different ways, depending on the fire behaviour model or management application. Within Australia, the management of fuels falls to the responsibility of state and territory jurisdictions and is undertaken by relevant land management and emergency response agencies within these areas (Hollis et al., 2011). Due to this and the number of different vegetation groups found across Australia, different methods of assessing fuels, used to derive values for input to fire behaviour models, have been developed. Common to most of these methods is the assessment of fuels within vertical structural layers called fuel strata (Hollis et al., 2015), as illustrated in Figure 1.1.2. The arrangement of fuel strata across a wildland is complex and dynamic. It varies with fuel group and responds to growth, decomposition and episodic disturbances (Hollis et al., 2015).
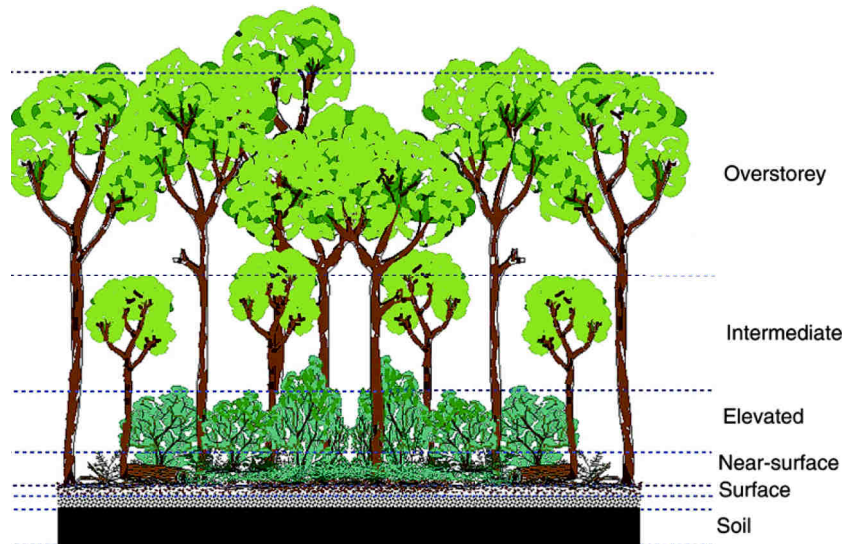
Figure 1.1.2: Illustrates the vertical structural layers, fuel strata, used in the assessment of fuel hazard. Source: Gould (2007).

Within each fuel strata the amount of biomass that is available to be consumed in a fire is quantified through fuel load. Fuel load is defined as dried mass per unit area, measured in $\frac{kilograms}{metre^2}$, or at larger scales $\frac{tonnes}{hectare}$ (Keane, 2015). This method is the most common way that fuel structure is quantified for a variety of fire behaviour models (McArthur, 1966a,b, 1967), as it directly relates available biomass to fire behaviour and can be assessed using common biomass estimation techniques (see Catchpole and Wheeler, 1992). The most accurate of these methods are destructive sampling techniques which require fuels to be sampled and oven dried to obtain direct biomass estimates (Keane, 2015). While the most accurate, when their use is extended to the landscape scale their precision decreases due to the small spatial extent for which they estimate fuel load (Gould and Cruz, 2012). In a land management setting, use of destructive sampling is also limited due to its labour intensity and implementation cost (Keane, 2015; Turner, 2007).

Recently, Hines et al. (2010) demonstrated that fuel load may not be the most robust determinant of fire behaviour, as for the same amount of fuel load available, a fire can behave differently based on varying fuel arrangement. Therefore, using fuel load homogenises different fuel arrangements, providing a poor indication of potential fire behaviour. In order to overcome the limitations of destructive sampling techniques and the use of fuel load, visual sampling techniques which estimate fuel hazard have been developed, respectively.

Fuel hazard is a rating on a five point scale representing the difficulty of fire suppression based on potential behaviour under first attack conditions (Hines et al., 2010; McCarthy et al., 1999). Fuel characteristics of an observed site are compared to descriptions which represent different fuel hazards (see Figure 1.1.1). A fuel hazard rating is determined for each strata, which are then combined to give an overall hazard rating for a sampled site (Hines et al., 2010; McCarthy et al., 1999; Gould et al., 2008). In this way, fuel hazard considers not only the amount of fuel but also its arrangement, providing a more robust indication of potential fire behaviour and suppression difficulty (Hines et al., 2010). It is also advantageous as fuel hazard

ratings either for individual strata or overall can be converted into fuel load estimates (Hines et al., 2010; McCarthy et al., 1999).

Table 1.1.1: Attributes used to assess elevated strata fuel hazard from the Overall Fuel Hazard Assessment Guide (Hines et al., 2010). Source: Hines et al. (2010).

Key attributes					Fuel Hazard Rating
Plant Cover	% dead	Vertical Continuity	Vegetation density	Thickness of fuel pieces	
<20% or low flammability species	<20%		Easy to walk in any direction without needing to choose a path between shrubs		Low
20-30%	<20%	Most of the fine fuel is at the top of the layer.	Easy to choose a path through but brush against vegetation occasionally.		Moderate
30-50%	<20%	Most of the fine fuel is at the top of the layer	Moderately easy to choose a path through, but brush against vegetation most of the time.		High
50-80%	20-30%	Continuous fine fuel from bottom to top of layer	Need to carefully select path through.	Mostly less than 1-2 mm thick.	Very High
>70%	>30%	Continuous fine fuel from the bottom to the top of the layer	Very difficult to select a path through. Need to push through vegetation.	Large amounts of fuel <2 mm thick.	Extreme

Visual assessment enables the rapid and nondestructive sampling and description of fuel hazard which can be tailored for different geographic regions and their specific fuel vegetation groups (Watson et al., 2012). Due to this, the use of visual estimation methods has become widespread by land managers within Australia (Hollis et al., 2015). However, while less limited than destructive methods, visual assessment techniques are also restricted in the spatial extent to which they can be implemented due their labour intensiveness, cost, and site accessibility (Watson et al., 2012). It has also been determined that visual assessment techniques suffer from assessor subjectivity. This variability of assessor subjectivity has been demonstrated by Gorrod and Keith (2009) using vegetation condition assessment protocols. Gorrod and Keith (2009) found an average coefficient of variation (CV) between assessment score of 15-18%. This is similar to Watson et al. (2012) who found a variation of 13%-21% between assessors for overall fuel hazard estimations.

1.1.4 Remote Sensing of Fuels

As with fire behaviour models, the assessment of fuels can be associated with the sophistication of the technology used to undertake them (see Section 1.1.2). Fuel assessment can now be carried out using Remote Sensing (RS) instruments such as satellite based optical systems or airborne laser systems. As RS insturments are are able to obtain information about objects without being in direct contact with them (Jensen, 2005), they have a number of advantages over field based techniques such as those described in Section 1.1.3. Remote Sensing instruments can obtain data over a greater spatial extent in a shorter time-frame, are cost-effective and can collect fuel data from regions inaccessible to humans (Frolking et al., 2009; Cash, 2012). In Australia, studies concerning fuel assessment using RS are limited, in number, the variety of RS instruments used, and fuel characteristics assessed (see Table 1.1.2). Arroyo et al. (2008) identify the potential of high resolution imagery, LiDAR, and the use of data fusion, which are either yet to be used or only have used been to a limited extent in Australia.

Table 1.1.2: Australian research which utilises RS instruments for fuel assessment.

Study	Title	Fuel Properties	Description
Brandis and Jacobson (2003)	Estimation of vegetative fuel loads using Landsat TM imagery in New South Wales, Australia	Fuel Load	Investigates the estimation of fuel loads using Landsat TM data based on equations describing litter accumulation and decomposition.
Caccamo et al. (2012)	Monitoring live fuel moisture content of heathland, Shrubland and sclerophyll forest in south-eastern Australia using MODIS data	Fuel Moisture	Investigates the use MODIS data and derived spectral indices to monitor live fuel moisture content of fire-prone vegetation types.
Cash (2012)	Assessing the capabilities of Landsat imagery for measuring fuel properties in Sydney Coastal Dry Sclerophyll Forest	Fuel Load	Investigates the use of Landsat TM derived spectral indices to estimate fuel load.
Chafer et al. (2004)	The post-fire measurement of fire severity and intensity in the Christmas 2001 Sydney wildfires	Fuel Load	Uses pre- and post-fire satellite imagery from SPOT2, to examine the fire severity and intensity of the Christmas 2001 wildfires in the greater Sydney Basin.
Haywood et al. (2010)	Fuel hazard mapping of the Victorian central highlands using LiDAR data	Fuel Hazard/ Load	Investigates the utility of LiDAR and Landsat TM data in retrospective fuel hazard mapping

High resolution imagery

High Resolution (HR) imagery is captured in the optical portion of the electromagnetic spectrum at resolutions ranging from ˜5 m to less than 1 m (Jensen, 2016). In their review, Arroyo et al. (2008) identifies that there are very few studies using HR imagery for fuel mapping, and that the levels of accuracy attained are comparable to those reported for lower resolution sensors. Since this review, only a single study has investigated the use of HR imagery for the assessment of fuel characteristics. Jin and Chen (2012) determined that the use of HR imagery provided improved estimates of total fine and total dead fuel loads when compared with coarser resolution Landsat imagery. It can therefore be seen that further investigation into the use of HR imagery for the assessment of fuel characteristics must be undertaken.

LiDAR

LiDAR emits and receives short bursts of laser energy that measure distance to target surfaces; which, when combined with Global Positioning Systems and Inertial Navigation Systems, allow the three dimensional coordinates of surfaces intercepted by the laser beam to be precisely computed. Their advantage over passive RS instruments is the ability to exploit gaps in canopy cover such that the vertical structure of sub-canopy vegetation can be sampled (Goodwin, 2006). This ability, which makes LiDAR ideal for the estimation of fuel hazard, has been demonstrated for retrospective fuel mapping by Haywood et al. (2010). Haywood et al. (2010) determined that LiDAR, fused with Landsat, can be used to generate estimates of fuel hazards efficiently and accurately over an extensive area.

Data Fusion

Data fusion is a data processing technique that deals with the association, correlation, and combination of information and data from different sources (Haywood et al., 2010). It is undertaken to obtain more information than could be provided by any single input dataset, considering only a minimum loss or distortion of data (Amarsaikhan et al., 2012). Haywood et al. (2010) and Garcia et al. (2011) demonstrate an example of this through the use of vertical vegetation structure measurements taken from LIDAR, and horizontal spectral measurements taken from a multispectral sensor. Data fusion can take a number of forms including pixel/data, feature, and decision fusion (Zhang, 2010).

1.2 Thesis Aims and Structure

The broad aim of this thesis is to investigate the use of RS to classify bushfire fuel hazard, which is motivated by the currently limited body of research concerning the use of RS to assess fuel characteristics within Australia (see Section 1.1.4, and Table 1.1.2). More specifically and directly, this thesis aims to address gaps identified by Cash (2012), who identified that; (a) more research needs to be done to test the ability of RS to measure fuel load with higher spatial resolutions, and (b) to determine if RS can measure fuel loads in multiple layers after fuel has had a long time to recover and accumulate. This thesis takes to form of two draft journal manuscripts with individual aims and objectives outlined in Table **??**. As previously outlined, fuel load does not account for the arrangement of fuels within a complex, which significantly affects fire behaviour (see Section 1.1.3). As well as this, when assessing fuel load one is unable to determine the load contribution from individual strata. For these reasons, this thesis will investigate the estimation of fuel hazard, rather than fuel load. As well as this, to address the temporal facet of (b) a study site which has not been significantly impacted by a fire event (>10 years), allowing fuels to recover and accumulate has been used. The Royal National Park, NSW Australia was suitably identified for this purpose.

The first paper, Chapter 2, is titled 'Estimating fuel hazard using optical datasets obtained at different times with pan-sharpening'. The aim of this chapter is to addresses (a) by investigating the potential to which pan-sharpening of high resolution ADS40 and Landsat 8 OLI imagery obtained at different times can be used to classify fuel hazard. The second paper, Chapter 3, is titled 'Classifying understory fuel hazard using LiDAR and high resolution imagery, integrating data fusion and machine learning'. The aim of this chapter is to address (b) by investigating the use of LiDAR, very high resolution imagery, data fusion and machine learning techniques to estimate understory fuel hazard in a wildland area. The final chapter of this thesis is a conclusion, synthesises the findings from both papers and suggests directions for future work.

Chapter 2 Estimating fuel hazard using optical datasets obtained at different times with pan-sharpening

Purpose

This chapter presents original research that has been undertaken entirely within this Master by Research program. This chapter provides an introduction, methods, results and discussion and conclusion pertaining to the estimation of fuel hazard using datasets obtained at different times with pan-sharpening. This chapter aims to investigate the potential to which pan-sharpening of high resolution ADS40 and Landsat 8 OLI imagery obtained at different times can be used to classify fuel hazard.

Format

In accordance with the Macquarie University policy for higher degree research thesis by publication[1], this chapter has been written for submission to a peer-reviewed journal, the International Journal of Wildland Fire. Repetition and any referencing and stylistic inconsistencies have been minimised to facilitate the thesis examination process. References from the paper and the literature review in the preceding chapter have been combined into one reference list provided at the end of the thesis.

Author contributions

Liam Turner (LT) carried out fieldwork and sampling, analysed all data, designed and drafted all figures and tables (except where acknowledged), wrote and edited the paper.
Hsing-Chung Chang (HC) provided comments on a draft of the paper, and supervised LT in the research.

Other significant contributions

William Farebrother (WF) undertook field sampling with LT and provided GIS technical advice
Sam Shumack (SS) assisted LT with the development of the IDL classification processing script, and provided ENVI and GIS technical advice

---

[1]The Macquarie University policy for thesis by publication states that a thesis may include a relevant paper or papers that have been published, accepted, submitted or prepared for publication for which at least half of the research has been undertaken during enrolment. The papers should form a coherent and integrated body of work. The papers are one part of the thesis, rather than a separate component (or appendix) and may be single author or co-authored. The candidate must specify their contribution and the contribution of others to the preparation of the thesis or to individual parts of the thesis in relevant footnotes/endnotes. Where a paper has multiple authors, the candidate would usually be the principal author and evidence of this should appear in the appropriate manner for the discipline. MQ Policy:
 http://www.mq.edu.au/policy/docs/hdr_thesis/policy.html

Abstract

Field based fuel asssesment methods are spatially restricted, costly, and the assessment of fuel load does not account for fuel particle arrangement. Although remote senisng insturments can overcome issues related to spatial extent, for temporally frequent instruments, this comes at the cost of low image resolution. To overcome this limitation, we used the Maximum Likelihood to classify fuel hazard from imagery and indices, derived using Gram-Schmidt pan-sharpening of ADS40 and Landsat 8 OLI imagery obtained at different times. The key findings from this study were: (i) no image resolution-independent image classification effect which could be attributed to pan-sharpening; (ii) low ($<1\%$/m) rates of change in accuracy/image resolution, inferring the plausibility of pan-sharpening as a method; (iii) fuel vegetation groups significantly affected the fuel hazard classification, and (iv) spectral indices provide no benefit for fuel hazard classification.

2.1 Introduction

Wildland fires are a major environmental issue in a wide range of ecosystems around the world (Arroyo et al., 2008). Accurate fuel maps are required for fire behaviour prediction and management of fuels at a variety of spatial and temporal scales (Arroyo et al., 2008). Fuel load is commonly used for mapping the distribution of fuels (Brandis and Jacobson, 2003; Cash, 2012; Chafer et al., 2004), however fuel load does not take into account the arrangement of fuels (Hines et al., 2010) which may lead to inaccurate fire behaviour predictions. Land managers commonly assess fuels in the field. While field based assessment is more accurate, this method is restricted in the spatial extent to which it can be implemented. This limitation can be overcome with Remote Sensing (RS). Although RS can provide greater coverage, for temporally frequent instruments, such as Landsat 8 OLI, this comes at the cost of low image resolution. For high resolution imagery the opposite relationship holds. To overcome this, the fusion of high resolution ADS40 and Landsat 8 OLI imagery obtained at different times through pan-sharpening, is proposed.

2.1.1 Fuel Hazard

Fuel is defined as any live or dead biomass available for combustion, which significantly influences the development and propagation of a fire (Hollis et al., 2015; Williams et al., 2012; Keane, 2015). The sum and arrangement of fuel in an area is termed a fuel complex (Watson, 2009). Within a fuel complex, a series of vertical structural layers known as fuel strata are often identified (Hollis et al., 2015; Watson, 2009). Fuel particles within each strata have a variety of characteristics which affect the way a fire behaves, including the thickness/fineness of fuel elements, mass of flammable material, live/dead fuel ratio, species composition, and arrangement of material (Watson, 2009; Roff et al., 2005; Keane, 2015). As there are several characteristics which contribute to a fires behaviour, fuels can be described in a number of ways. Historically, empirical fire behaviour models (those commonly used in Australia), required the dry mass of fuels (fuel load) as input to represent the magnitude of available fuels within a complex (McArthur, 1958, 1960, 1966*b*, 1967). However as demonstrated by Hines et al. (2010),

for the same available fuel load a fire can behave differently based on fuel particle arrangement. To describe fuels so that fuel particle arrangement is accounted for, the concept of fuel hazard has been developed (McCarthy et al., 1999; Hines et al., 2010; Watson, 2009). Fuel hazard is a rating on a five point scale for each contributing fuel stratum representing the difficulty of fire suppression based on potential behaviour under first attack conditions (Hines et al., 2010). Fuel hazard considers not only the amount of fuel but also its arrangement. It provides a more robust indication of potential fire behaviour and suppression difficulty (Hines et al., 2010). Describing fuel with fuel hazard is also advantageous as rating levels can be transformed into a fuel load values which incorporate vertical structure, in order to create products for fire behaviour simulations (Hines et al., 2010).

2.1.2 Fuel Vegetation Groups

Wildland vegetation coalesces into similar forms (structures and arrangements) based on topography, micro and macro climatic conditions, access to water and various other factors. In order to catalogue vegetation, Keith (2004), provides a comprehensive description of vegetation forms in NSW. In the context of fire behaviour, these forms are termed fuel vegetation groups, and are defined as an identifiable association of fuel elements of distinctive species, form, size, arrangement and continuity that will exhibit characteristic fire behaviour under defined burning conditions (Merrill and Alexander, 1987). Within Australia, a number of discrete fire behaviour models exist, for fuel vegetation groups which frequently burn including forests, grasslands, and shrublands (which include heathlands) (Cruz et al., 2015). While they are distinct, Watson (2009) identifies that fuel vegetation groups can occur within a matrix of other vegetation types such as heathlands within dry sclerophyll forests, and as such, tend to burn at the same time. Coastal heathlands are particularly fire prone and exhibit unique properties such as well aerated fuel and the tendency of dead foliage, which contains flammable oils and waxes, to persist on plant. As a result, when heathlands are encountered by a spreading fire, they may significantly change the nature of its behaviour. Understanding the unique fuel hazard that each fuel group presents is important for the planning and implementation of fuel management strategies and to model fire behaviour.

2.1.3 Remote Sensing of Fuel Characteristics

While the most accurate method for the assessment of fuel characteristics is field based (Keane, 2015), implementing field based methods at large spatial scales can be time-consuming and costly (Cash, 2012). In order to overcome this, Remote Sensing (RS) instruments, which can obtain data over a greater spatial extent, in a shorter amount of time, and at lower cost, have been used to estimate fuel characteristics (Cash, 2012). Within Australia only a few studies have used coarse to medium resolution optical instruments to assess fuel characteristics including fuel load (Brandis and Jacobson, 2003; Chafer et al., 2004; Cash, 2012) and fuel moisture (Caccamo et al., 2012).

Within these studies spectral indices, products derived from combinations of individual bands of multispectral RS instrument, are also used to assess fuel characteristics (Cash, 2012). Healthy vegetation reflects more in the Near Infrared (NIR) part of the electromagnetic spec-

trum due to intra leaf scattering, and absorbs in the red and blue parts of the spectrum due to photosynthetic pigments found in chlorophyll (Cash, 2012). The most commonly used, are broadband greenness indices such as Simple Ratio (SR), and Normalised Difference Vegetation Index (NDVI). These indices measure the quantity, health, and condition of vegetation (Cash, 2012), and therefore can be used for the assessment of fuel characteristics. Other indices developed on SR and NDVI, are more sensitive in high biomass regions and less sensitive to atmospheric effects, for example, the Enhanced Vegetation Index (EVI) and Atmospherically Resistant Vegetation Index (ARVI), respectively. Unlike SR and NDVI, these indices are yet to be used for the purposes of fuel assessment.

Although RS instruments have been used to assess fuel characteristics the potential of very high resolution imagery has not yet been explored in depth (Arroyo et al., 2008). Only a single study, Jin and Chen (2012), has investigated the use of high resolution imagery for the assessment of fuel characteristics. Jin and Chen (2012) determined that the use of high resolution imagery provided improved estimates of total fine and dead fuel loads when compared with coarser resolution Landsat imagery. This demonstration motivates the investigation of the use of high resolution imagery for fuel hazard mapping.

2.1.4 Data Fusion

Remote sensing instruments record data in a variety of configurations determined by the portion of the electromagnetic spectrum they observe, how often they record new data, their location above the ground, and sensor characteristics (Ghassemian, 2016). Integrating data from different instruments and configurations can provide greater insight about features on the ground than may otherwise be achieved through the use of a single sensor. This process, termed data fusion, is undertaken to obtain more information, with minimal loss or distortion of data (Amarsaikhan et al., 2012). Data fusion also enables the use of datasets recorded at different resolutions and times. This is advantageous as datasets recorded by RS instruments are either of high spatial resolution and low temporal frequency or vice versa. This is due to both the geometry of satellites in orbit and the cost of airborne RS. Arroyo et al. (2008) identified that the use of multiple data sources represents a promising approach in remote sensing for fuel mapping. Although RS data fusion can be performed in a number of ways (see Amarsaikhan et al., 2012; Zhang, 2010; Ghassemian, 2016) pixel level fusion, which combines raw data from multiple sources into single dataset, is particularly useful. As pixel-level fusion can enhance structural and textural details while retaining the spectral fidelity of input data (Zhang, 2010).

2.1.5 Research Aims and Objectives

The aim of this study is to investigate the potential to which pan-sharpening of high resolution ADS40 and Landsat 8 OLI imagery obtained at different times can be used to classify fuel hazard. More specific objectives are to: i) investigate the data fusion effect, independent of resolution, of pan-sharpening on fuel hazard classification, ii) determine if pan-sharpening can be used to improve the resolution of fuel hazard classification both overall and for each fuel hazard class, and iii) examine the influence of fuel vegetation groups on the classification of fuel hazard

2.2   Methods

2.2.1 Study Area

This study was done in the Royal National Park (RNP) in New South Wales, Australia. The RNP covers 13, 348 ha of land and is locatec adjacent to the Tasman Sea and the southern fringe of metropolitan Sydney (see Figure 2.2.1). It has a varied topography consisting of ridges and valleys on the western side of the park, and a coastal plateau towards the eastern side of the park (see Figure 2.2.1). The park contains a rich floristic diversity including several types of rainforest, freshwater swamps and estuarine wetlands (National Parks & Wildlife Service NSW, 2000), and is dominated by dry sclerophyll forest and coastal heathlands (See Figure 2.2.1).

The fire history of the park has been recorded and mapped since 1965. Since this time, the largest fires recorded occurred in 1993 and 2001, burning approximately 97.9% and 59.6% of the park respectively. Historically, most frequent pattern of fire spread is for fires to enter the from the west and north-west sides of the park; which sit adjacent to areas of public access (National Parks & Wildlife Service NSW, 2000). At the time of this study, the majority of vegetation within the park had not been burnt for a period of approximately 15 years.
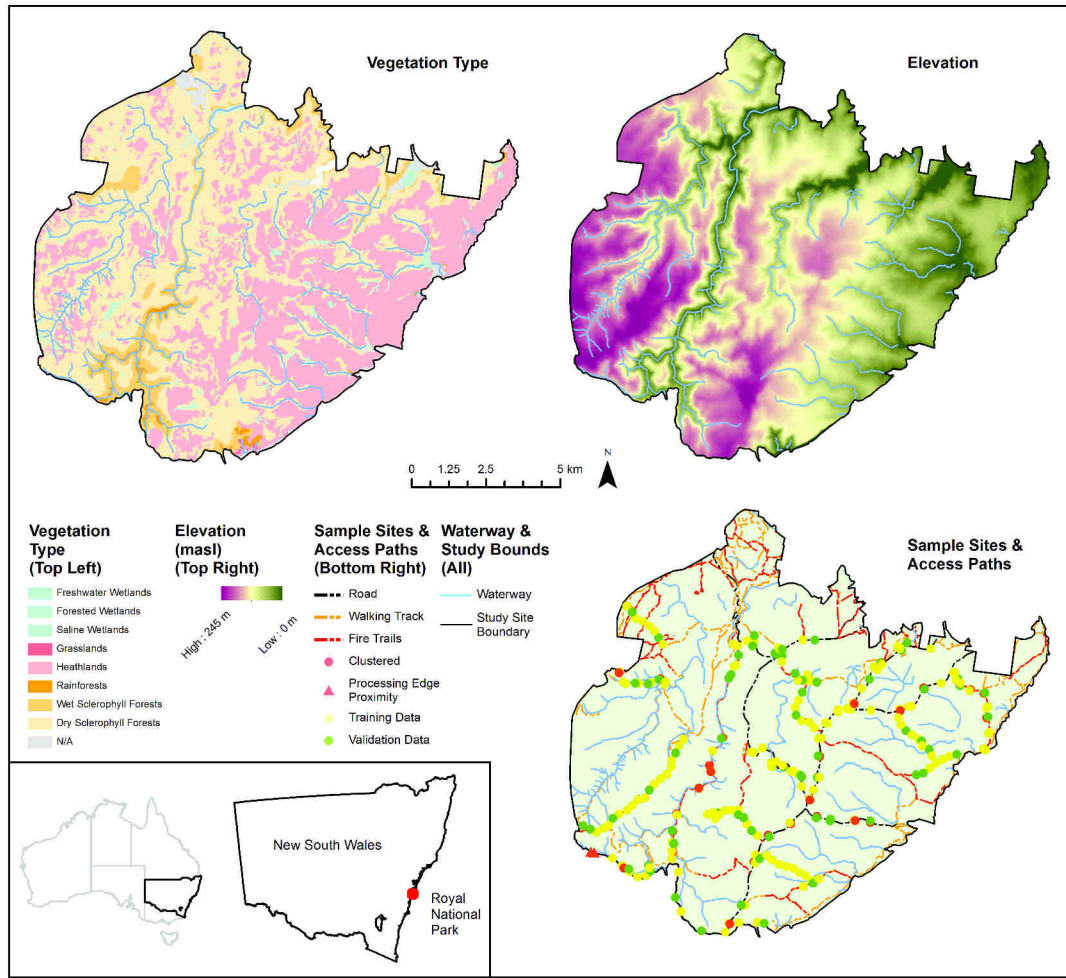
Figure 2.2.1: Map of the study site. Bottom left (inset): Location of the RNP along the NSW coast. Top left: the dominant vegetation types occurring in the RNP (Land & Property Information NSW, 2013). Top right: topography of the RNP (Geoscience Australia, 2015). Bottom right: location of study sampling sites and access paths (Office of Environment & Heritage NSW, 2016).

2.2.2 Datasets

Field Data

Field data used to train and validate the image classifications for this analysis was collected by two assessors during April and June 2016. Fuel hazard levels were visually assessed within a 20 m radius using the Overall Fuel Hazard Assessment Guide 4th Ed (OFHAG) (see Table 2.2.1)(Hines et al., 2010). Visual assessment was chosen as it is a low cost, rapid, and non-destructive technique (Brandis and Jacobson, 2003). Sites were chosen in the field, separated by approximately 250 m along walking accessible paths including fire trails, tracks, and when safely accessible, roads. At each site, assessors walked into the vegetation from the access path for a minimum of 20 m (the assessment radius), or as far as safely possible. This was done to minimise any path edge effects and ensure assessors viewed a significant portion of the vegetation associated with each site (Gould and Cruz, 2012). To minimise any structural sampling bias, sites were located on alternating sides of accessed paths. These paths were chosen within the constraints of time and to obtain a dataset with comprehensive spatial coverage. During fieldwork in April, sites were assessed for some paths in a spatially clustered manner;

assessors pushed into alternate sides of the path from the same point. This clustering could not be achieved during the June portion of fieldwork due to time constraints brought about by severe weather, and dataset spatial coverage. The location of each site was also recorded using a Garmin 72H GPS with an accuracy variance of within 10 m.

Table 2.2.1: Summary of fuel characteristics and the stratum for which they were recorded at each sampling site site.

Stratum	Height	Characteristics Assessed
Canopy	> 4 m	Canopy Base Height, Canopy Top Height
Elevated	1-4 m	% Cover, % Dead, Average Height (m), Elevated Fuel Hazard (1-5)
Near Surface	0-1 m	% Cover, % Dead, Average Height (cm), Near Surface Fuel Hazard (1-5)
Surface	0 m	% Cover, Average Depth (mm), Surface Fuel Hazard (1-5)
Bark		Stringy Hazard (0, 2-5), Ribbon Hazard 0, 2-5), Other Hazard (1-3)

Recorded sample site locations were imported into ArcGIS (ESRI, 2011) and buffered with a 30 m radius, to incorporate the GPS inaccuracy. Due to the clustered sampling regime, paired sites with overlapping buffers were observed (see Figure 2.2.1). As each site had unique fuel hazard values, the site from each overlapping pair furthest from the accessed path was retained in order to maximise the size of the dataset and minimise edge effects. Sites were also removed where proximal to the processing extent due to processing edge effects (2 sites), and where duplicate assessment occurred for calibration purposes (2 sites). From the 249 field sites, selective site removal resulted in 219 buffered areas, with a total area of 61 ha equivalent to approximately 0.5% of the study area (see Figure 2.2.1).

To produce datasets for classification training and validation, the buffered areas were split into training (70%) and testing (30%) datasets using random selection stratified across the fuel hazard ratings to ensure a balanced representation of each class was in the derived datasets. This was done with the Sample Design Tool (Buja, 2015) in ArcGIS (ESRI, 2011).

To investigate the classification of overall fuel hazard for different fuel vegetation groups, the field site buffers were intersected with a native vegetation dataset obtained from the Land Property Information NSW (LPI, 2013) . Areas were assigned the majority fuel group that fell within them. The fuel vegetation groups with the requisite number of samples to produce a validation classification, >10n per class (n number of layers) (Jensen, 2016), were Dry Sclerophyll Forests, and Heathlands. The samples for each of these structures were then separated into balanced training and testing datasets using the method described.

Remote Sensing Data

The imagery used for this study was acquired by the LPI as a part of their Standard Coverage Program in March 2008 (Land & Property Information NSW, 2008). The image (referred to as ADS40 image) was created by ortho-rectifying, colour matching and joining overlapping image strips captured on 30/3/2008 with multiple flight lines using a Leica ADS40 airborne digital sensor (Land & Property Information NSW, 2008). The ADS40 image was provided by the vendor as a Standard Colour (three band, red green blue) Orthorectifed Mosaic in the ECW file format, with a ground sample distance of 50 cm (Land & Property Information NSW, 2008).

A cloud free Landsat 8 OLI scene, taken closest to the second period of field data was downloaded from USGS Earth Explorer (USGS, 2016). Although the field data was recorded in two separate time periods, the remotely sensed phenological variation between these periods was low, and there were no significant disturbances such as fire affecting imagery texture. Remotely sensed phenological variation was determined to be low due to a strong correlation ($R^2_{adj} = 0.94$) of NDVI pixel values from images taken closest to each of the field data collection periods (see Appendix 1). Therefore, rather than analyse two separate Landsat images, analysis of single scene was deemed appropriate. Use of a single scene also mitigated the temporal break up of the training/validation dataset, which might introduce bias. Before analysis, the Landsat 8 OLI scene was pre-processed within ENVI 5.3 (Exelis Visual Information Solutions, 2016*a*) using the Radiometric Calibration tool and FLAASH atmospheric correction tool. The Landsat 8 OLI scene, calibration and correction details are outlined in Table 2.2.2.

Table 2.2.2: A summary of the Landsat 8 OLI scene, radiometric calibration, and atmospheric correction details.

Landsat Scene	Radiometric Calibration	Atmospheric Correction
Sensor: Landsat 8 OLI	Algorithm: ENVI	Algorithm: FLAASH
ID: LC80890842016206LGN00	Radiometric Calibration	Atmospheric Model:
Capture Date: 24/7/2016	Calibration: Radiance	Mid Latitude Winter
Path 89 / Row 84	Interleave/Type:	Aerosol Model:
Resolution: 30 m	BIL/Float	2 Band over water
Bands: 7	Scale Factor: 0.10	Aerosol Retrieval: Maritime

2.2.3 Data Fusion

Gram-Schmidt pan-sharpening was used as a data fusion method for this study. Gram-Schmidt pan-sharpening is a intensity modulation algorithm (Zhang, 2010; Jawak and Luis, 2013) which uses a generalised principle component orthogonalisation procedure (Ghassemian, 2016) to create a set of non- or less correlated components from input datasets (Amarsaikhan et al., 2012). This algorithm was chosen for implementing and as it is characterised by high fidelity in rendering the spatial details in the fused product (Ghassemian, 2016). It has also been identified as having the most comprehensive performance when compared to a number of other pan-sharpening methods (Jawak and Luis, 2013).

For pan-sharpening, a pan-chromatic image at high resolution is required. For this study, a synthetic panchromatic image was derived from the ADS40 image by taking the mean of the three bands supplied at their native resolution 50 cm (see 2.2.2). To determine if pan-sharpening can be used to improve the resolution of fuel hazard classification both overall and for each fuel hazard class, this image was resampled out to 1, 2, 5, 10, 15, 20, 25, and 30 m resolutions, respectively. Each resampled synthetic panchromatic ADS40 image was then fused within the SPEAR Pan-sharpening Tool in ENVI 5.3 (Exelis Visual Information Solutions, 2016*a*).
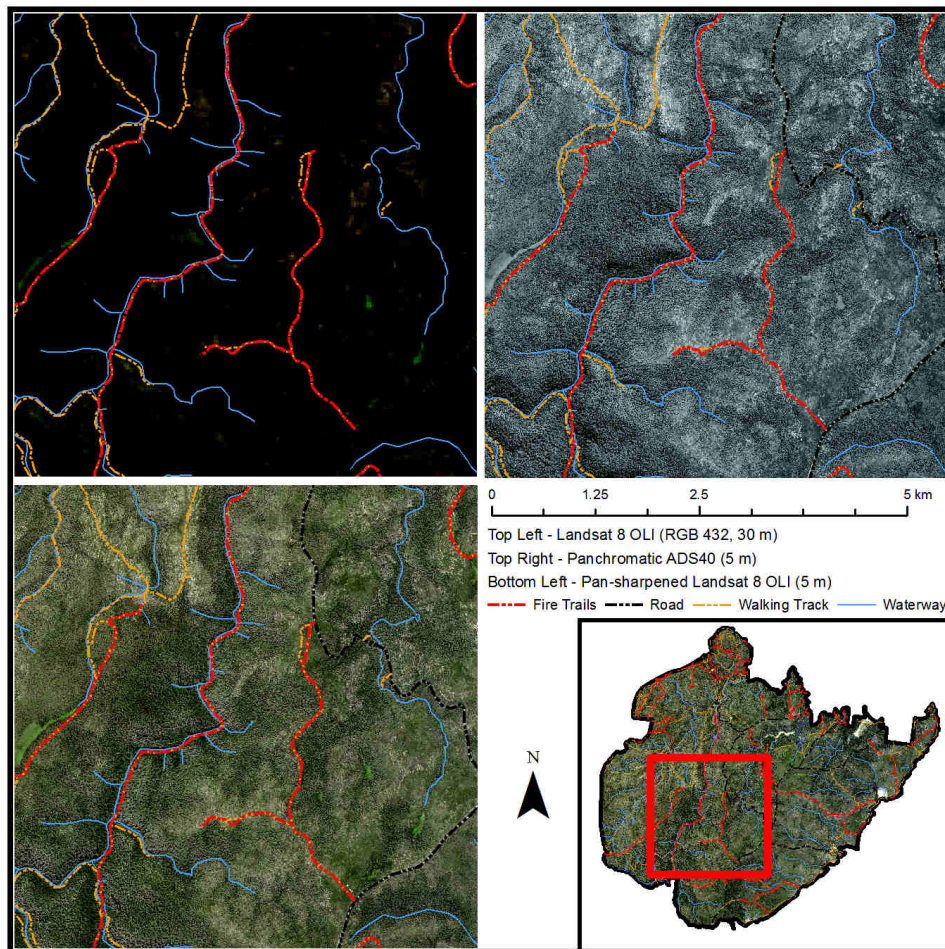
Figure 2.2.2: Pan-sharpening inputs and output. Bottom right (inset): full study site extent, and extent of zoomed images. Top right: input ADS40 panchromatic image at 5 m resolution. Top left: input Landsat 8 OLI image, at 30 m resolution. Bottom left: output pan-sharpened Landsat 8 OLI image, at 5 m resolution.

2.2.4 Spectral Indices

To further investigate the effect of data fusion, a number of spectral indices were derived from both the Landsat 8 OLI image at its native resolution, and for each resolution of the pan-sharpened images. The spectral indices calculated for this study are outlined in Table 2.2.3. Simple Ratio (SR) and Normalised Difference Vegetation Index (NDVI) were chosen as they are the most commonly used spectral indices derived from RS instruments, and have been used previously to assess fuel characteristics (Chafer et al., 2004; Cash, 2012; Brandis and Jacobson, 2003). While functionally these indices are similar, NDVI is more commonly used as it does not suffer from multiplicative noise issues such as illumination differences, cloud shadows, atmospheric attenuation, or topographic variation (Cash, 2012). Comparing the results derived from these indices should then give an indication of whether these issues are affecting the classification of fuel hazard. For this reason, two other spectral indices, Atmospherically Resistant Vegetation Index (ARVI) and the Enhanced Vegetation Index (EVI), were also computed. Atmospherically resistant vegetation index is an enhanced version of NDVI which is more resistant to atmospheric factors making it useful in regions of high atmospheric aerosol content such as coastal regions (Kaufman and Tanre, 1992). Enhanced vegetation index was developed as an improvement of NDVI, which is optimised for dense vegetation conditions (Jensen, 2016). This makes EVI suitable for the assessment of the fuel vegetation groups considered in this study (see Section 2.1.2).

Table 2.2.3: Summary of spectral indices used in this investigation

Spectral Index	Formula	Description
Simple Ratio (SR)	$SR = \frac{Red}{NIR}$	A ratio of wavelengths with highest reflectance for vegetation (NIR) and the deepest chlorophyll absorption (Red) (Birth and McVey, 1968).
Normalised Difference Vegetation Index (NDVI)	$NDVI = \frac{(NIR-Red)}{(NIR+Red)}$	Similar to SR, it's formulation and use of the highest absorption and reflectance regions of chlorophyll make it robust over a wider range of conditions (Rouse Jr et al., 1974).
Enhanced Vegetation Index (EVI)	$EVI = 2.5 \left(\frac{NIR-Red}{NIR+(6*Red)-(7.5*Blue)+1} \right)$	Developed to optimise vegetation signal with improved sensitivity in high biomass regions through a de-coupling of the canopy background signal (Huete et al., 2002).
Atmospherically Resistant Vegetation Index (ARVI)	$ARVI = \frac{NIR-[Red-\gamma(Blue-Red)]}{NIR+[Red-\gamma(Blue-Red)]}$ where $\gamma = 1$	An enhanced NDVI less sensitive to atmospheric effects, due to correction for molecular scattering and ozone absorption (Kaufman and Tanre, 1992; Jensen, 2016).

2.2.5 Image Classification

For this analysis, Maximum Likelihood Classification (MLC) was used to classify the image pixels into fuel hazard ratings. Maximum likelihood classification is a commonly used supervised image classification algorithm which utilises probability density functions to assign classes, based on the pixels in the images used to train the algorithm (James, 2013). Each image or index produced has been grouped into an image set determined by whether or not pan-sharpening has been applied. Along with this, a comparison image set, comprising of the original ADS40 RGB imagery and derived panchromatic ADS40 imagery at the processing resolutions was also produced.

Image classification was done using IDL 8.5 (Exelis Visual Information Solutions, 2016b), and accuracy assessment undertaken using the 'validate()' function from the RStoolbox package based in the R statistical computing language (R Development Core Team, 2008; Leutner and Horning, 2016). The validity of each classification, and therefore the ability to estimate fuel hazard, was assessed using Overall Accuracy (OA%) which represents the number of correctly classified pixels (the diagonal of the confusion matrix), divided by all pixels that have been classified (Huete et al., 2002; Jensen, 2016). A summary of the input images and details of the training and validations datasets used for classification are summarised in Tables 2.2.4 and 2.2.5.

Table 2.2.4: The derivation and grouping of imagery and indices into comparison, non-pan-sharpened, and pan-sharpened image sets.

Image Set	Resolution (m)	Derivation	Image/Index
Comparison	1, 2, 5, 10, 15, 20, 25, 30	Obtained Dataset	ADS40 RGB
		Mean ADS40 RGB	ADS40 Panchromatic
Non-pan-sharpened	30	Corrected Landsat 8 OLI	Landsat 8 OLI
		Corrected Landsat 8 OLI	NDVI, SR, EVI, ARVI
Pan-sharpened	1, 2, 5, 10, 15, 20, 25, 30	Corrected Landsat 8 OLI	Landsat 8 OLI
		Pan-sharpened Landsat 8 OLI	NDVI, SR, EVI, ARVI

Table 2.2.5: The distribution of sampling sites amongst fuel vegetation groups and fuel hazard ratings. The distribution is stratified across fuel hazard ratings within each fuel group. * Other are sampling points that fell into any other vegetation type, such as rainforests or wetlands.

Fuel Vegetation Group	Total	Training					Total	Validation					Total
		No. of Samples per Hazard Rating Class						No. of Samples per Hazard Rating Class					
		Low	Moderate	High	Very High	Extreme		Low	Moderate	High	Very High	Extreme	
All	219	8	16	29	54	46	153	3	7	13	23	20	66
Dry Schlerophyll	94	4	6	15	25	16	66	2	3	6	10	7	28
Heathland	99	3	8	6	24	28	69	1	3	3	11	12	30
Other*	26												

2.2.6 Analysis

The processing steps to derive the fuel hazard classification results for this study are illustrated in Appendix 2. The results of this analysis are presented as three sections addressing the objectives in Section 2.1.5. The Data Fusion Section investigates the data fusion effect, independent of resolution, of pan-sharpening on fuel hazard classification. While the Accuracy and Resolution section seeks to determine if pan-sharpening can be used to improve the resolution of fuel hazard classification both overall and for each fuel hazard class. The influence of fuel vegetation groups on the classification of fuel hazard is examined simultaneously through these sections.

Data Fusion

To investigate the effect of data fusion, all images and indices at 30 m resolution (that of the Landsat 8 OLI image pan-sharpening input) from the comparison, non-pan-sharpened, and pan-sharpened image sets are used (see Table 2.2.4). The results of this investigation also establish a control, to which the results of other investigations in this study can be compared.

Accuracy and Resolution

The desired outcome of the use of data fusion is to at best improve, or at worst, incur only a small (but known) loss in fuel hazard accuracy with increasing resolution. To determine if the data fusion method of pan-sharpening achieves this outcome, the OA% results of the comparison and pan-sharpened image sets are plotted against the resolutions at which they have been produced (1, 2, 5, 10, 15, 20, 25, 30 m, respectively). The quality, magnitude and direction of the relationship for each image or index is quantified by fitting a linear model to obtain the R^2_{adj} and model equation, respectively. The R^2_{adj} statistic quantifies the quality of the relationship, while the slope of the fitted line shows the how OA% changes with pan-sharpened image resolution (OA% vs m-resolution). This shows the degree to which pan-sharpening achieves the desired outcome.

Fuel Class

To make decisions concerning the implementation fuel management techniques it useful to know more accurately where fuel hazard may meet or exceed maximum fuel threshold. For this, the accuracy for each fuel hazard classification is more critical than the OA%. The accuracy for each fuel hazard class can be determined by calculating the User and Producer accuracies. These accuracies are calculated across the rows and down the columns of a classification matrix, and represent the classified fuel hazard rating commission and omission accuracy, respectively. The User and Producer accuracies have been calculated for both for all images and indices across image sets and resolutions, and presented for all 30 m images (similar to the Data Fusion section), and then increasing resolution (similar to the Accuracy and Resolution section). For the purposes of visualisation the accuracies have been binned into ranges of 10%.

2.3 Results

Across all imagery assessed in this study the OA was low, <50% OA. The best performing model achieving an accuracy of 43% for heathlands using pan-sharpened Landsat 8 OLI image at 30 m resolution.

2.3.1 Data Fusion

The effect of data fusion was investigated through the classification of all 30 m resolved imagery from each of the images sets derived for this analysis (see Table 2.2.4). The results of these classifications are illustrated in Figure 2.3.1. Within this figure a wide variance of results is observed, that is, no single effect or trend which may be attributed to pan-sharpening, can be identified.
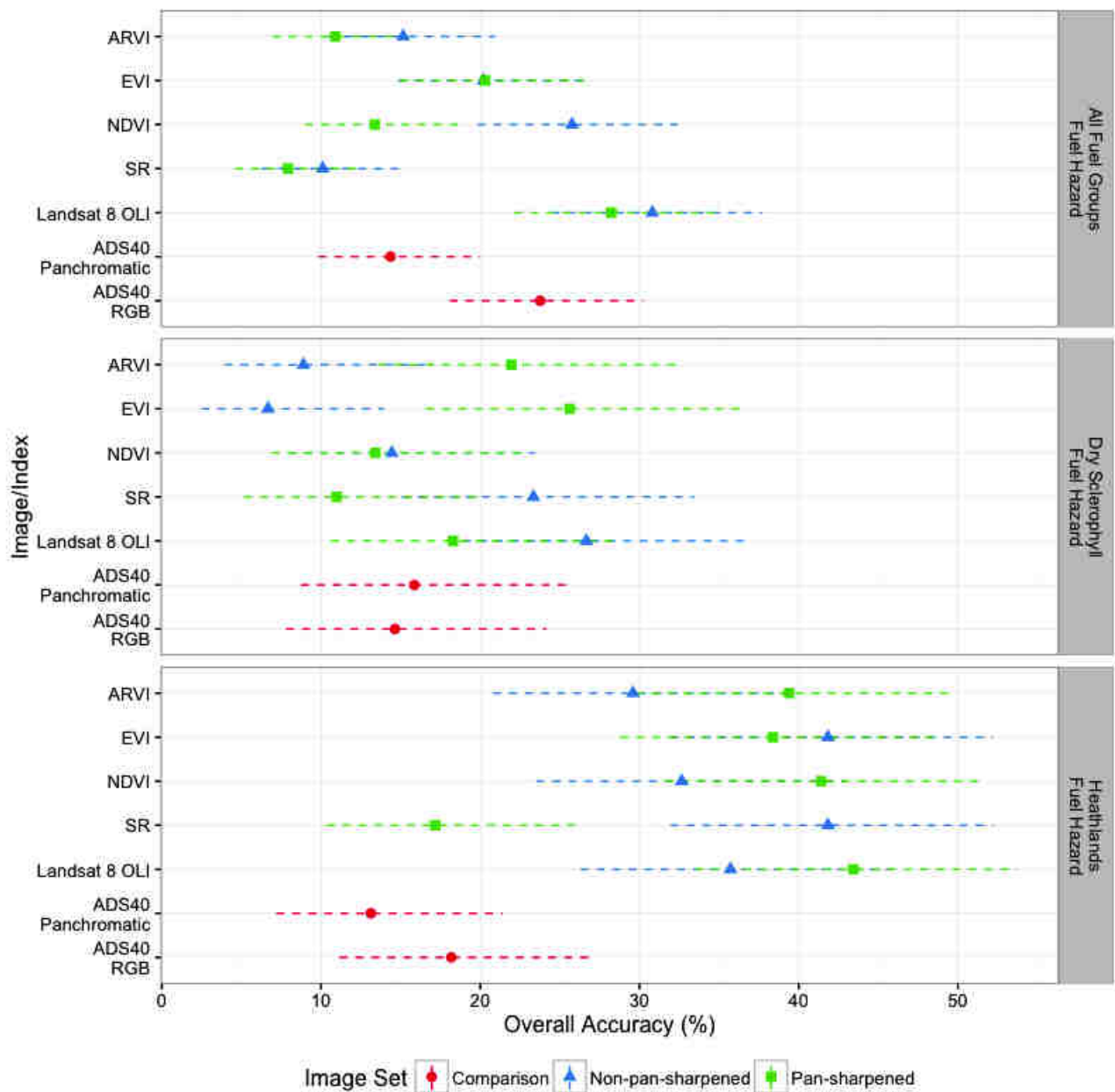
Figure 2.3.1: Image classification results of the Data Fusion section for each fuel group. Confidence intervals (95%) are displayed as dashed lines.

What can be discerned is the greater ability of both non-pan-sharpened and pan-sharpened imagery to classify fuel hazard for the heathlands fuel group. This is hypothesised to be caused by the relative openness of heathland vegetation to dry sclerophyll which has greater canopy closure. This closure is thought to obfuscate the spectral signal from understory vegetation structures resulting in a loss in classification accuracy (Cash, 2012; Goodwin, 2006).

Comparing the indices within Figure 2.3.1, there is no clear distinction concerning the ability to classify fuel hazard, regardless of fuel vegetation group, between those indices which are optimised (EVI, ARVI), and those which are not (SR, NDVI). It was also evident that these indices do not ever outperform some form of the Landsat 8 OLI imagery (either non-pan-sharpened, or pan-sharpened). It is suggested that this is due to the reduced dimensionality of the indices, which surmise data from the Landsat 8 OLI imagery. From this, and the lack of any distinct trends in the data it is hypothesised that the results, for imagery and indices are detecting signals which are biased by the sampling method and design rather than the inherent fuel hazard distribution.

2.3.2 Accuracy and Resolution

Overall, there is a significant degree of variability in the quality of the fitted linear models, with R^2_{adj} ranging from -0.17 to 0.9 (on a possible scale of 0-1^2) in Figure 2.3.2.

The best model fit acheived with pan-sharpened Landsat 8 OLI imagery for all fuel vegetation groups ($R^2_{adj} = 0.9$). From Figure 2.3.2, it can be seen that the magnitude of the OA% vs m-resolution is low, <1 OA% vs m-resolution. There was also large variation in the direction (sign of OA% vs m-resolution value) of the fitted models, when examined across the imagery types and fuel vegetation groups.

2.3.3 Fuel Class

Results to determine whether pan-sharpening can be used to improve the resolution of fuel hazard classification for each fuel hazard class are illustrated in Figure 2.3.3 for the non-pan-sharpened imagery at 30 m resolution, and 2.3.4 for pan-sharpened imagery across all resolutions produced (comparison image set results are also included in each of these figures). When fuel classes were examined using non-pan-sharpened imagery at 30 m resolution, a maximum of up to three fuel hazard rating classes were predicted better than 10% (Figure 2.3.3). In more than half the cases, these are hazard ratings greater than or equal to High. However, there is no consistency either across the images, or fuel vegetation groups. For the Producer accuracy, the results were much more variable. However, some classes were classified with high accuracy (e.g. EVI achieves a $(90, 100]$ $OA\%$ for Very High fuel hazard, and all fuel vegetation groups).

When examined across pan-sharpened imagery resolution for imagery type and fuel group (Figure 2.3.4), no clearly definable trend is exhibited. Very High and Extreme fuel hazard ratings are the most consistently classified, with relatively higher User-Producer accuracies than other rating classes. Similarly, the Low fuel hazard rating has the poorest classification consistency, never reaching a User or Producer accuracy greater than 10%.

---

[2]Negative R^2_{adj} values occur where the fit model is worse than would be otherwise achieved by fitting a straight line.
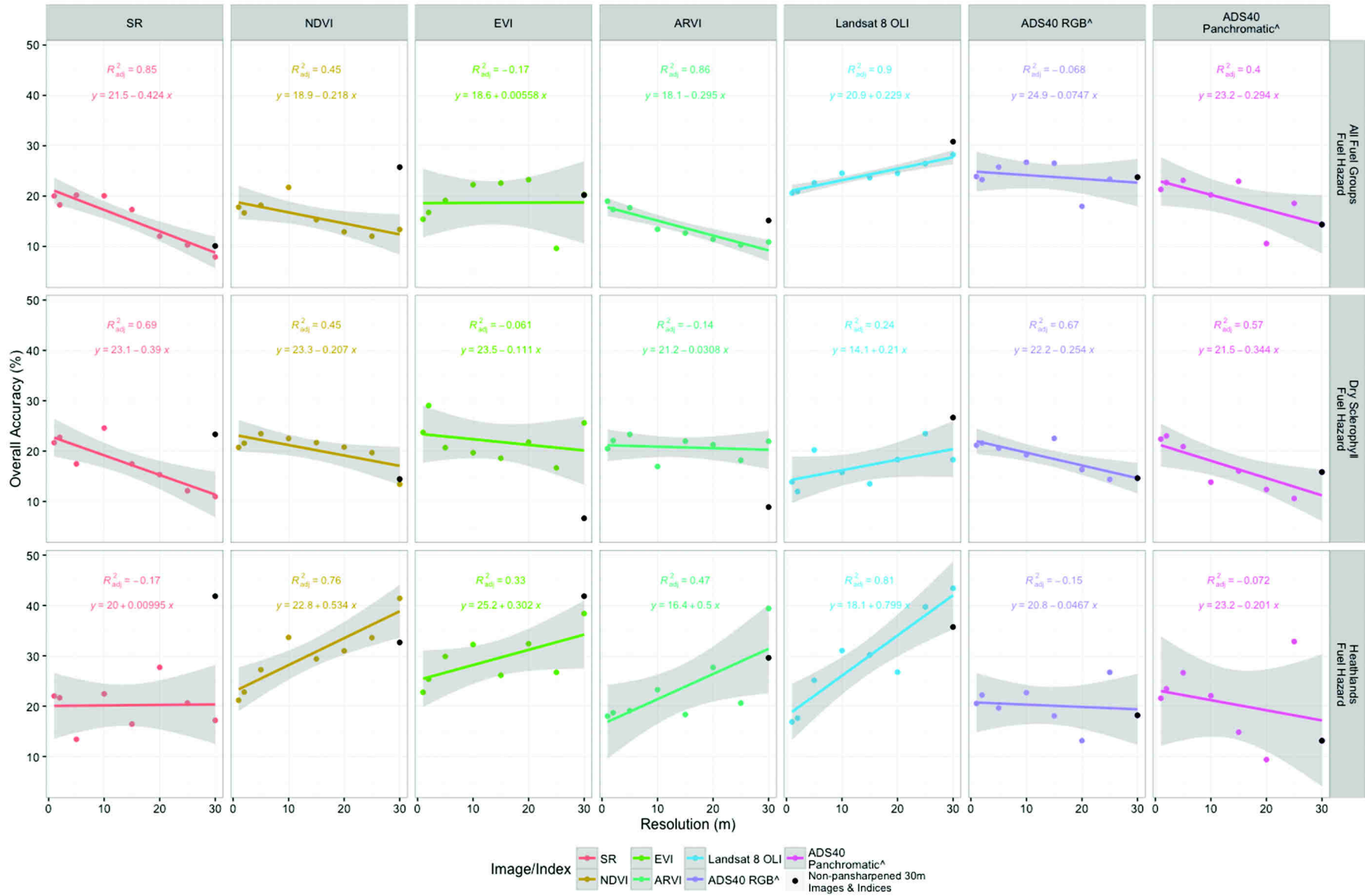
Figure 2.3.2: Image classification results of Accuracy and Resolution section. For comparison the results non-pan-sharpened images at 30m resolution are also plotted. Results from the Comparison image set denoted by ^. Shown in grey are the confidence intervals (95%) for each linear model.

Figure 2.3.3: Fuel Class section for Comparison (denoted by ^) and non-pan-sharpened image sets at 30 m resolution.
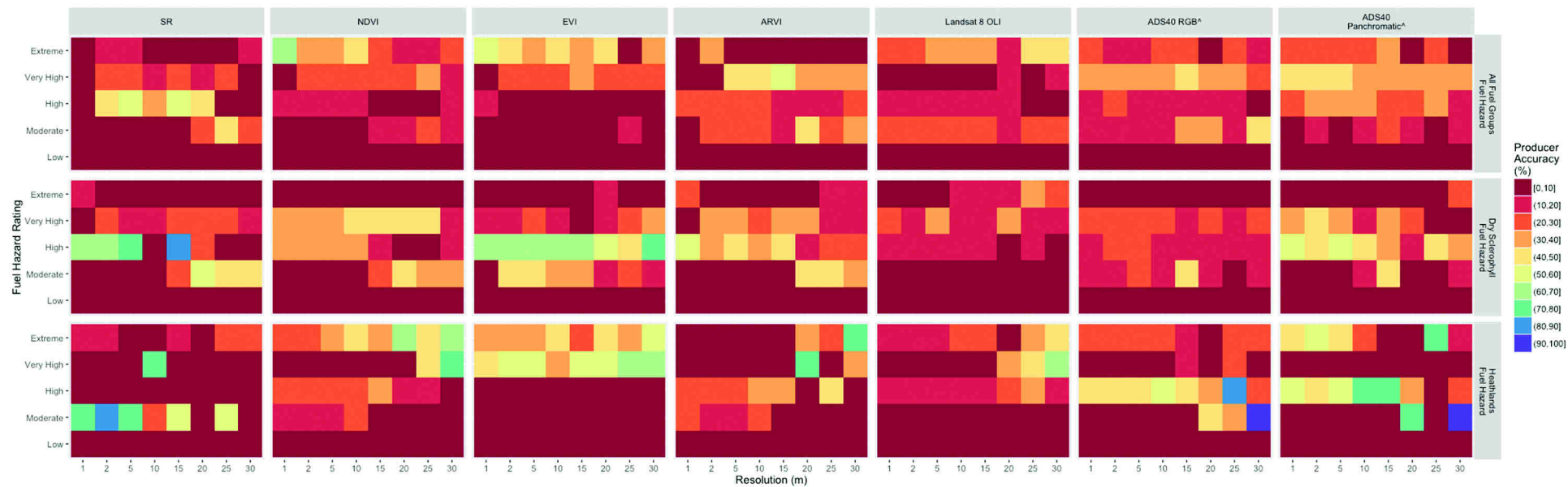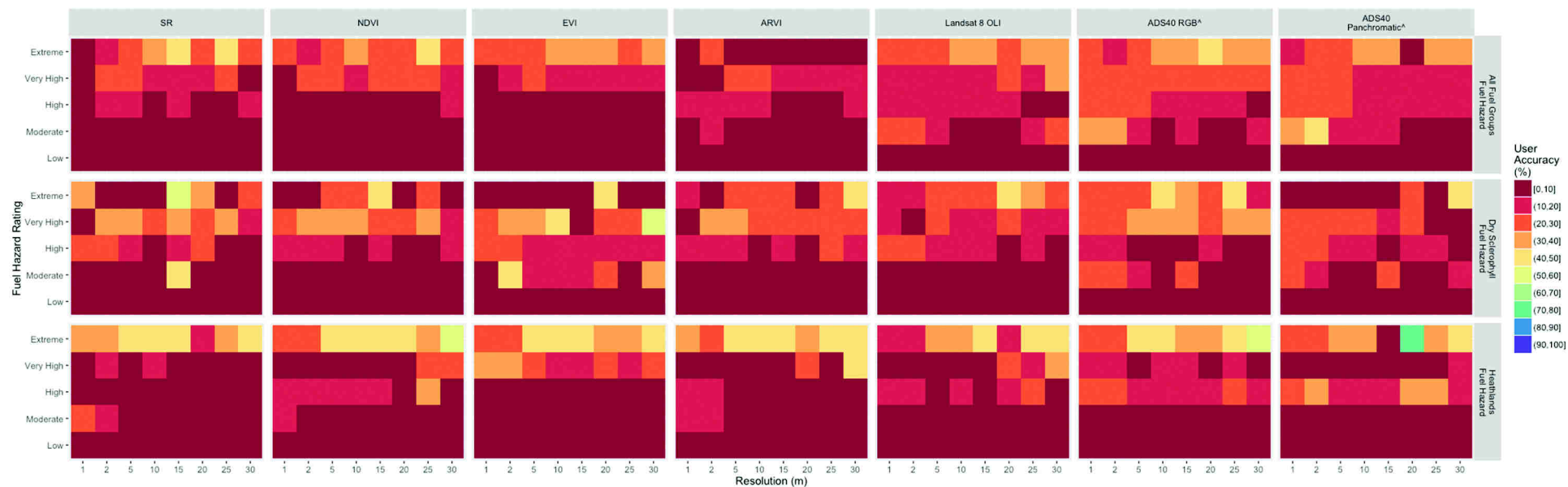
Figure 2.3.4: Fuel Class section for Comparison (denoted by ^) and pan-sharpened image sets plotted against image resolution.

2.4 Discussion

There are a number of issues which affect the results of this study. These issues include various facets of the field data and its collection including its location accuracy, the sample radius, sampling design and method, the nature of the data fusion method used, and the classification method.

Pixels used to train and validate fuel hazard classification models were taken from each image using a 30 m buffer around each site assessed in the field. This buffer incorporated both the accuracy of the GPS used to collect the location of the sites (10 m) and the radius over which fuel hazard was assessed (30 m). While this area is suitable for the assessment of fuel in the field, it can be seen that by incorporating GPS accuracy in this way, the assessment area is synthetically enlarged such that pixels are included in these areas which have not been assessed, introducing error. In addition, the area of assessment is kept fixed and has not been scaled relative to the resolution of the images used. This is hypothesised to introduce spectral signal noise within the assessment areas as the image resolution increases, acting to obfuscate MLC.

The sampling design and method are also hypothesised to introduce error into the collected field data. Field sites for this study were located, in a clustered manner during the initial period of collection and a non-clustered manner in the secondary period of collection (see Section 2.2.2). Field based sample site allocation, rather than pre-determined site allocation resulted in a variable number of data points for each fuel hazard class. Due to the limited number of points collected and the large number removed as part of the field data pre-processing (See Section 2.2.2) it was not possible to further remove points to normalise the training/validation data. It is also hypothesised that normalising the data in this way would remove the representation of fuel hazard distribution that is inherent in the data. It can be seen from the results of the fuel hazard classification (Section 2.3.3) that the data would have benefited from being normalised, as not normalising the dataset resulted in significant errors of omission and commission for each fuel hazard rating. Similarly, due to the number of overlapping points removed, spatially clustered data points had to be retained to meet the amount of data required for classification. This clustering is hypothesised to bias the sampled spectral signal representative of each fuel hazard. Resulting in the training data not being representative of the study area. It can also be seen that splitting the data into training and testing datasets (rather than using other methods such as cross-validation) may act to further bias the dataset by training on spatially clustered points which may have a similar spectral signal, and then testing on points which have a different spectral signal but the same fuel hazard rating.

The visual estimation method used in this analysis is hypothesised to introduce error into this analysis as a result of assessor subjectivity. Watson et al. (2012) determined that visual estimation methods can be susceptible to as much as 15% variability between assessors in their rating of fuel hazard. This, in conjunction with a limited number of calibration points between assessors, an ill-defined assessment radius, and significant difference in assessor height (~165 cm, and ~197 cm respectively), are thought to compound error for the fuel hazard ratings recorded

in this study. As well as this, there is no way to validate the way this visual estimation method captures the variability of fuel hazard over the scale considered in this analysis.

The errors introduced by the sampling method and design are hypothesised to be amplified when used as inputs for MLC. This is due to MLC assuming that input datasets are normally distributed. In future work, alternative classification methods which are not restricted by assumptions of normality or linear decision boundaries such as a Support Vector Machine are suggested.

The direct fusion of the two datasets introduces error due to possible image misregistration, as well as spatial and spectral distortions introduced by pan-sharpening. Pan-sharpening is more commonly used with datasets from the same sensor, which are inherently spatially registered and have the same sensor characteristics such as optical distortions and sensitivity. Due to this, pan-sharpening does not consider local dissimilarities between images, which can result in significant spectral and spatial distortions when images from difference sensors are used. These distortions may be further amplified where datasets are spatially and spectrally misregistered. For this analysis, as the images were not taken at the same time and the apparatus to validate and correct the spatial registration of the imagery (to the minimum resolution used i.e. 1 m) was unavailable. Only a superficial assessment of the registration (through visual inspection) was undertaken.

This study demonstrated that there is limited benefit for the use of spectral indices, as indicated by the greater performance of the non- or pan-sharpened Landsat 8 OLI imagery over any of the derived indices (see 2.3.1). This is attributed to the greater dynamic range of the imagery compared to the spectral indices. This greater dynamic range is suggested to provide more information for the classification algorithm to delineate fuel hazard classes. In addition, other studies have shown that the effectiveness of the use of indices can vary between conditions including location, level of cover, and sensor used; even within similar environmental regions (Cash, 2012).

Due to the limited literature concerning the assessment of fuel characteristics within Australia. The results of this study are only comparable to one other. In estimating fuel load for the purposes of retrospective fire severity mapping, using Landsat derived NDVI image and 166 sample sites dominated by Dry Sclerophyll forest; Chafer et al. (2004) obtained $R^2 = 0.43$ in the Metropolitan and Woronora water supply catchments near Sydney. For the purposes of comparison, fuel hazard and fuel load are considered analogous. It can be seen in this study for the Dry Sclerophyll fuel group, that non-pan-sharpened NDVI achieved an OA% of 14.4%. Although assessing fire severity, Chafer et al. (2004) used similar sampling methods and design to this study. Due to this similarity, the relative difference in inaccuracy is suggested to be caused, in this study, by the inclusion the GPS inaccuracy in the field site buffers, and the use of non-normalised data in conjunction with MLC.

2.5 Conclusion

While methods used in this study incur a number of limitations, there was evidence inferring plausible use of pan-sharpening to improve the resolution of imagery and indices for fuel hazard classification. Pan-sharpening imagery has a number of advantages including the ability to arbitrarily improve image resolution with a known and quantified effect on classification accuracy. Improving the resolution at which fuel hazard is classified would also enable an increase in the spatial precision of fire behaviour modelling. This would inform a more detailed understanding of the risks imposed by potential fire behaviour, which has a number of advantages for research and land management.

This study also presents evidence that the classification of fuel hazard is influenced by the structure of the vegetation within the fuel vegetation groups investigated. Particularly high canopy closure is hypothesised to obfuscate the spectral signal from understory vegetation structures decreasing fuel hazard classification accuracy

2.5.1 Future Work

It is suggested that future work investigate the relationship between canopy cover, fuel group, and fuel hazard, so that canopy cover measurements, which can also be derived from remotely sensed imagery such as Foliage Projective Cover, could be integrated into the method. Future work should also investigate the temporal relationship between the input datasets, to determine whether the degree of structural change over time in the absence of significant disturbance plays a role in fuel hazard classification accuracy. In this way, the temporal extent of the difference between input imagery sets could be determined.

More broadly, further investigation into the relationship between field based fuel assessment methods and remotely sensed datasets needs to be undertaken. It is proposed that visual estimation methods needs to be be more rigorously developed, both in terms of method and design. Increased robustness in the use of visual estimation methods with remotely sensed datasets will be advantageous in both management and research settings, and at various spatial scales. An example of how they might be improved is through the integration of visual obstruction methods (Davies et al., 2008) which directly quantify vegetation structure, and not limited by assessor subjectivity. As well as developing specific sampling design schema, such as those used in fractional cover methods (Muir et al., 2011), that are spatially scalable.

2.6 Acknowledgements

2.7 References

See combined reference list at the end of the thesis.

Chapter 3 Classifying understory fuel hazard using LiDAR and high resolution imagery, integrating fusion and machine learning

Purpose

This chapter presents original research that has been undertaken entirely within this Master by Research program. The chapter provides an introduction, methods, results and discussion and conclusion pertaining to classifying understory fuel hazard using LiDAR and high resolution imagery, integrating fusion and machine learning. This chapter aims to investigate the use of LiDAR, very high resolution imagery, data fusion and machine learning techniques to estimate understory fuel hazard in a wildland area.

Format

In accordance with the Macquarie University policy for higher degree research thesis by publication[1], this chapter has been written for submission to a peer-reviewed journal the Journal of Applied Remote Sensing. Repetition and any referencing and stylistic inconsistencies have been minimised to facilitate the thesis examination process. References from the paper and the literature review in the preceding chapter have been combined into one reference list provided at the end of the thesis.

Author contributions

Liam Turner (LT) carried out fieldwork and sampling, conducted all and mapping, analysed all data, designed and drafted all figures and tables, wrote and edited the paper.

Hsing-Chung Chang (HC) developed the study with LT, provided comments on a draft of the paper, and supervised LT in the research.

Other significant contributions

William Farebrother (WF) undertook field sampling with LT, and provided GIS technical advice

---

[1]The Macquarie University policy for thesis by publication states that a thesis may include a relevant paper or papers that have been published, accepted, submitted or prepared for publication for which at least half of the research has been undertaken during enrolment. The papers should form a coherent and integrated body of work. The papers are one part of the thesis, rather than a separate component (or appendix) and may be single author or co-authored. The candidate must specify their contribution and the contribution of others to the preparation of the thesis or to individual parts of the thesis in relevant footnotes/endnotes. Where a paper has multiple authors, the candidate would usually be the principal author and evidence of this should appear in the appropriate manner for the discipline. MQ Policy:
http://www.mq.edu.au/policy/docs/hdr_thesis/policy.html

Abstract

Understory fuel strata contain the most important source of fuels which contribute the most to the rate of spread and flame height of a wildland fire. By managing these fuels, the difficulty of fire suppression and likelihood of an uncontrollable crown fire breaking out is minimised, reducing the risk a fire posed to people and the environment. Traditionally, fuel assessment is field based, which is time-consuming and costly. While optical remote sensing instruments have been used, they are unable to directly quantify the hazard of understory fuels due to canopy obstruction. This study aimed to use LiDAR, high resolution imagery, data fusion and machine learning classification techniques to estimate understory fuel hazard within a wildland area. Key findings were: that the combined use of LiDAR point elevation and intensity metrics provide the most accurate classification of understory fuel hazard, and although statistical fusion through principal component analysis achieved the highest classification accuracy, the simplest form of data fusion image stacking provided a more consistent improvement of accuracy.

3.1 Introduction

Fire is a principle wildland disturbance that shapes the landscape mosaic and influences biogeo-chemical cycles (Hermosilla et al., 2014). To develop and implement fire management strategies an understanding of the spatial distribution of fuels is essential (Arroyo et al., 2008).

The understory strata contains the most significant source of fuels (Cheney, 1994; Goodwin, 2006). These fuels burn in the continuous flaming zone at the edge of a fire contributing the most to its rate of spread and flame height (Hines et al., 2010). Cheney (1994) showed that independent crown fires are unlikely to occur where there is a lack of understory fuels as crown fires are produced by convection pre-heating from ignited understory fuels. Therefore, if the amount of understory fuels can be managed, the difficulty of fire suppression and likelihood of an uncontrollable crown fire breaking out is minimised, in turn, reducing the risk a fire posed to people and the environment.

3.1.1 Fuel Assessment

Traditionally, the spatial distribution of fuels has been assessed using field based techniques such as destructive sampling or visual estimation (McCarthy et al., 1999; Hines et al., 2010; Ferster and Coops, 2014; Davies et al., 2008). While field based methods are the most accurate techniques (Keane, 2015), at larger spatial and temporal scales they become time-consuming and costly to implement (Keane et al., 2001; Rollins et al., 2004; Arroyo et al., 2008; Cash, 2012). To overcome these limitations, Remote Sensing (RS) instruments, which are able to obtain data at a greater spatial extent and temporal frequency with a relatively lower cost, have been applied to estimate fuel distribution (Frolking et al., 2009; Cash, 2012). Within Australia, passive optical RS instruments have been used to estimate fuel properties across all vegetation strata. These properties include fuel load (Brandis and Jacobson, 2003; Chafer et al., 2004; Cash, 2012), fuel moisture (Caccamo et al., 2012) and post-fire vegetation regrowth (Jacobson, 2010). While these properties can be used to inform management practices, when estimated using optical RS instruments they are inferred rather than direct measurements. This

inference is due to the inability of these sensors to detect the contribution of fuels from strata below the canopy when overstory coverage is high (Keane et al., 2001; Garcia et al., 2011).

3.1.2 LiDAR

Light Detection and Ranging (LiDAR) is becoming an effective alternative for overcoming the previously described limitations of optical RS, as it can be used to estimate the structure of fuels beneath the canopy (Keane et al., 2001; Chuvieco and Kasischke, 2007; Arroyo et al., 2008). LiDAR is an active RS technique which utilises distance measurements of laser pulses to produce highly accurate, precisely georeferenced, three dimensional point representation of a scanned surface (Lefsky et al., 1999; Baltsavias, 1999; Ediriweera et al., 2014; González-Ferreiro et al., 2014). In forested areas, most pulses are reflected back to the sensor from leaves and branches of the vegetation canopy. However, as the canopy is not an opaque/impermeable surface and its magnitude of cover can vary with vegetation composition, pulses are able to penetrate and reflect back to provide measurements of understory structure (González-Ferreiro et al., 2014).

Due to the large data volume (greater than tens of millions of points at the landscape scale) and high dimensionality (multiple recorded returns, each with x- y- z- locations and intensity per emitted pulse), the raw LiDAR point cloud is precluded from direct use in modelling algorithms (Zhao et al., 2011). Therefore, metrics which summarise point characteristics are commonly derived for use in analysis. These metrics are grouped into point elevation based metrics which summarise the distribution of elevation amongst points (Garcia et al., 2011) and point intensity based metrics which summarise the backscattered energy from scanned objects (González-Ferreiro et al., 2014). Point elevation metrics are more commonly used, as the point cloud data from which they are derived is not affected by atmospheric issues common to other remote sensors such as illumination differences, clouds and shadows. Intensity metrics are less commonly used as their signal can be affected by factors such as terrain properties, and flight and sensor characteristics (González-Ferreiro et al., 2014). Although suffering from these problems the use of intensity metrics for the characterisation of fuels in the context of fuel hazard is motivated, as the sensor operates in the Near InfraRed (NIR) part of the electromagnetic spectrum. The NIR portion of the spectrum is commonly used to characterise the 'greenness' or productivity of vegetation through spectral indices (Cash, 2012). As the intensity values recorded by a LiDAR sensor lay within the NIR portion of the spectrum these values may then be used as a proxy for the productivity of vegetation, or the ratio of dead/live fuel when considered in the context of fuel assessment.

3.1.3 Data Fusion

Data fusion deals with the association, correlation and combination of information and data from different sources (Haywood et al., 2010). Fusing data from different sources can occur in a number of ways from simple image stacking, termed data type fusion, to more advanced statistical fusion techniques such as Principle Component Analysis (PCA), and Minimum Noise Fraction (Mutlu et al., 2008), termed statistical fusion. A number of studies (Erdody and Moskal, 2010; Garcia et al., 2011; Jakubowksi et al., 2013; Kane et al., 2014; Nordkvist et al.,

2012) have shown that combining LiDAR data with other data sources can improve the accuracy of results, compared to those individual input data sources (Garcia et al., 2011). For the study presented here, fusing LiDAR and imagery will take advantage of the vertical structure information from the LiDAR and the horizontal multispectral information from the optical data (Garcia et al., 2011).

3.1.4 Machine Learning

To produce and assess the validity of maps which portray the spatial distribution of fuels, image classification techniques are commonly used. Supervised classification or Machine Learning (ML) algorithms are a subset of these techniques which apply statistical learning methods to a set of training data, to quantify the functional relationship between the observations within a dataset to make inferences or predictions about other unseen datasets (Lary et al., 2016). These ML algorithms are known as 'universal approximators' (Lary et al., 2016) and are ideal for addressing non-linear systems and situations where there is incomplete theoretical knowledge but for which a significant number of observations exist (Lary et al., 2016).

In general ML algorithms are either, parametric or non-parametric based on the nature of the assumptions they hold about input datasets. Parametric algorithms summarise data with a set of parameters using a predefined functional form (James, 2013). These algorithms have traditionally been used in RS analysis for the classification of imagery, as they are quick to run, the resultant parameters easy to understand, and the functional form is known (Hsu et al., 2010). However they are limited by the predefined functional form which may not fit the relationship under investigation (James, 2013). Non-parametric ML algorithms overcome this limitation by not making explicit assumptions concerning the nature of the functional form, and instead seek its estimation (James, 2013).

3.1.5 Research Aims and Objectives

The overall aim of this study is to to investigate the use of LiDAR, very high resolution imagery, data fusion and machine learning techniques to estimate understory fuel hazard in a wildland area. In order to achieve this aim a number of more specific objectives are to: i) investigate the ability to use LiDAR point and intensity metrics for understory fuel hazard estimation, ii) compare the effects of data fusion methods, and iii) compare/contrast the accuracy of different machine learning algorithms for the estimation of understory fuel hazard

3.2 Materials and Methods

3.2.1 Study Area

This study was done in the Royal National Park (RNP) in New South Wales, Australia. The RNP covers 13, 348 ha of land and is located adjacent to the Tasman Sea and the southern fringe of metropolitan Sydney. It has a varied topography consisting of ridges and valleys on the western side of the park, and a coastal plateau towards the eastern side of the park (See Figure 3.2.1). The park contains a rich floristic diversity including several types of rainforest, freshwater swamps and estuarine wetlands (National Parks & Wildlife Service NSW, 2000), and is dominated by dry sclerophyll forest and coastal heathlands (See Figure 3.2.1).

The fire history of the park has been recorded and mapped since 1965. Since this time, the largest fires recorded occurred in 1993 and 2001, burning approximately 97.9% and 59.6% of the park respectively. Historically, the most frequent pattern of fire spread is for fires to enter the from the west and north-west sides of the park; which sit adjacent to areas of public access (National Parks & Wildlife Service NSW, 2000). At the time of the study, the majority of vegetation within the park had not been burnt for a period of approximately 15 years.
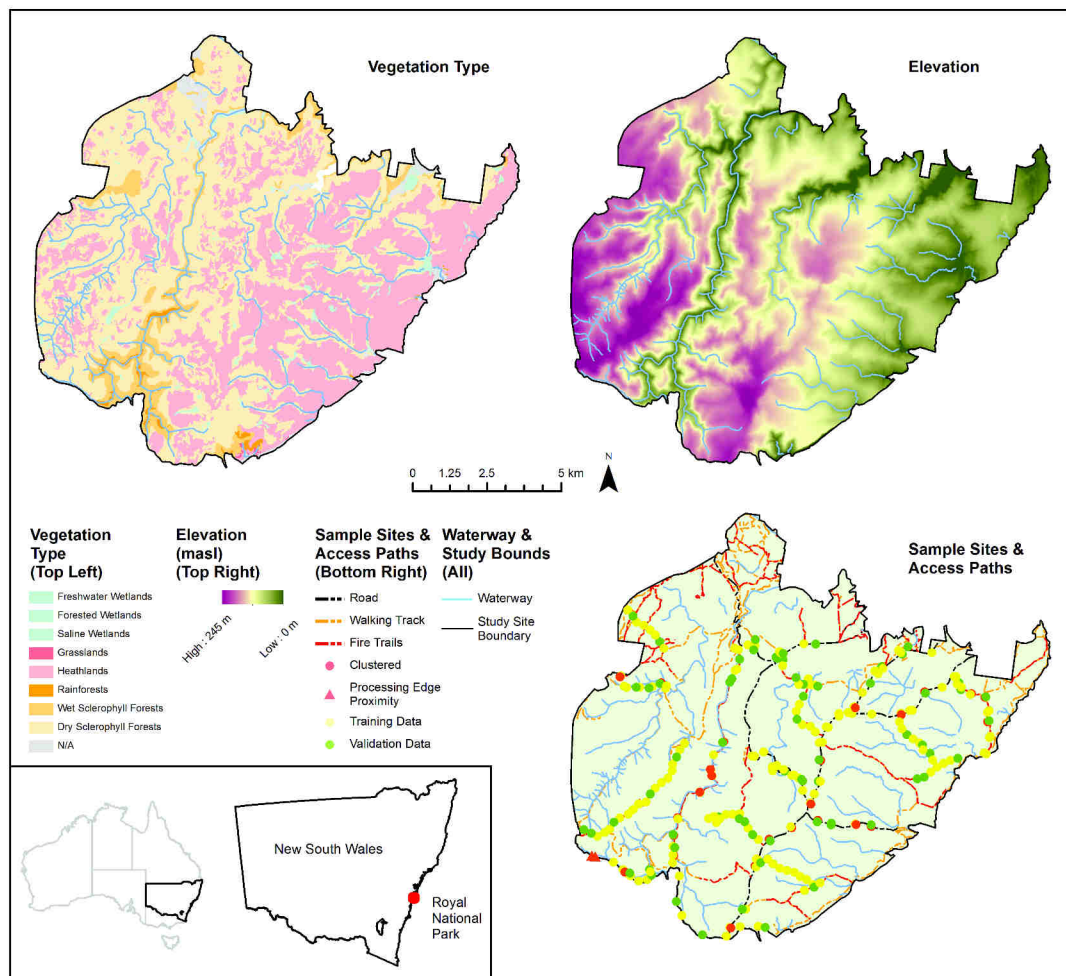
Figure 3.2.1: Map of the study site. Bottom left (inset): Location of the RNP along the NSW coast. Top left: the dominant vegetation types occurring in the RNP (Land & Property Information NSW, 2013). Top right: topography of the RNP (Geoscience Australia, 2015). Bottom right: location of study sampling sites and access paths (Office of Environment & Heritage NSW, 2016).

3.2.2 Data

Field Data

Field data used to train and validate the image classifications for this analysis was collected by two assessors during April and June 2016. Fuel hazard levels of Near Surface and Elevated fuel strata were visually assessed within a 20 m radius using the Overall Fuel Hazard Assessment Guide 4th Ed (OFHAG) (see Table 3.2.1)(Hines et al., 2010). Visual assessment was chosen as it is a low cost, rapid, and non-destructive technique (Brandis and Jacobson, 2003). Sites were chosen in the field, separated by approximately 250 m along walking accessible paths including fire trails, tracks, and when safely accessible, roads. At each site assessors walked into the vegetation from the access path for a minimum of 20 m (the assessment radius), or as far as safely possible. This was undertaken to minimise any path edge effects and ensure assessors viewed a significant portion of the vegetation associated with each site (Gould and Cruz, 2012). To minimise any structural sampling bias, sites were located on alternating sides of accessed paths. These paths were chosen within the constraints of time, and in order to obtain a dataset with comprehensive spatial coverage. During the April fieldwork, sites were assessed for some paths in a spatially clustered manner; assessors pushed into alternate sides of the path from the same point. This clustering could not be achieved during the June portion of fieldwork due to time constraints brought about by severe weather, and dataset spatial coverage. The location of each site was also recorded using a Garmin 72H GPS with an accuracy variance of within 10 m.

Recorded sample site locations were imported into ArcGIS (ESRI, 2011) and buffered with a 30 m radius, in order to incorporate the GPS inaccuracy. Due to the clustered sampling regime, paired sites with overlapping buffers were observed (see Figure 3.2.1). As each site had unique fuel hazard values, the site from each overlapping pair furthest from the accessed path was retained in order to maximise the size of the dataset and minimise edge effects. Sites were also removed where proximal to the processing extent due to processing edge effects (2 sites), and where duplicate assessment occurred for calibration purposes (2 sites). From the 249 sites sampled in the field, this resulted in 219 buffered areas, with a total area of 61 ha equivalent to approximately 0.5% of the study area (see Figure 3.2.1).

Table 3.2.1: Summary of fuel characteristics and the stratum for which they were recorded at each sampling site site.

Stratum	Height	Characteristics Assessed
Canopy	> 4 m	Canopy Base Height, Canopy Top Height
Elevated	1-4 m	% Cover, % Dead, Average Height (m), Elevated Fuel Hazard (1-5)
Near Surface	0-1 m	% Cover, % Dead, Average Height (cm), Near Surface Fuel Hazard (1-5)
Surface	0 m	% Cover, Average Depth (mm), Surface Fuel Hazard (1-5)
Bark		Stringy Hazard (0, 2-5), Ribbon Hazard 0, 2-5), Other Hazard (1-3)

Imagery and LiDAR

Imagery and LiDAR were provided by the Land & Property Information, NSW (LPI). An ADS40 image captured on 30/3/2008 by the LPI as a part of their Standard Coverage Program in March 2008 (Land & Property Information NSW, 2008) was provided as a Standard Colour (Red (R), Green (G), Blue (B)) Orthorectifed Mosaic in ECW file format, with a ground sample distance of 50 cm.

A LiDAR point cloud acquired by LPI in May 2011 using a Leica ALS50-II sensor was provided by the vendor in LAS 1.2 file format classified to the C3 standard with a horizontal accuracy of 0.8 m, and a vertical accuracy of 0.3 m (Land & Property Information NSW, 2011; Intergovernmental Committee on Surveying & Mapping, 2010). This dataset contained four return values with an average point density of 1.62 per square metre.

3.2.3 LiDAR Metrics

Before metrics could be derived the LiDAR point cloud was topographically normalised, by subtracting the elevation of a DEM derived from all ground classified points. Normalisation is necessary so that the x- y- z- locations within the point cloud represent the height above the ground rather than height above sea level. This was done using the LasHeight algorithm within ERDAS Imagine 2015 (Hexagon Geospatial, 2015; Isenberg, 2016).

For this study, both point elevation and point intensity metrics were derived using univariate first and second moment summary statistics (Jensen, 2016) (see Table 3.2.2). A height bin metric, defined as the number of points that fall within a discrete height range divided by the total number of points that within each cell, which describes the percentage of cover within the height bin, were also derived (Heritage and Large, 2009).

Both elevation and intensity metrics were produced using the r.in.lidar tool in GRASSGIS (GRASS Development Team, 2016) from the normalised height cloud. A processing resolution of 5 m was chosen so that a sufficient number of points were available to compute each metric and provide an accurate representation of cover within each height bin (Garcia et al., 2011). Missing values that occurred within the metrics were removed using a conditional 3x3 focal mean filter. All metrics and the respective R, G, B ADS40 bands (once resampled to 5 m) were then standardised by taking their Z score (Equation 3.2.1). This standardisation is necessary in order to avoid metrics with greater numeric ranges dominating those with smaller ranges which could bias results during data fusion and machine learning (Hsu et al., 2010; Garcia et al., 2011).

$$Z\,Score = \frac{x - \bar{x}}{stddev(x)} \tag{3.2.1}$$

Table 3.2.2: Summary of the LiDAR metrics derived in this investigation.

Metric	Type	Description	Fuel Strata Height (m)	Reference
Coefficient of Variation	Point/ Intensity	Surface roughness	Elevated: 1-4 Near Surface: 0-1	Garcia et al., 2011 Erdody and Moskal, 2010 Ediriweera et al., 2014 González-Ferreiro et al., 2014 Kramer et al., 2014
Mean	Point/ Intensity	Mean Point Elevation for Fuel Strata	Elevated: 1-4 Near Surface: 0-1	Garcia et al., 2011 Erdody and Moskal, 2010 Hermosilla et al., 2014 Ediriweera et al., 2014 Andersen et al., 2005 Kramer et al., 2014
Standard Deviation	Point/ Intensity	Standard Deviation of point elevation	Elevated: 1-4 Near Surface: 0-1	Garcia et al., 2011 Jakubowksi et al., 2013 Hermosilla et al., 2014 Ediriweera et al., 2014 González-Ferreiro et al., 2014 Kramer et al., 2014
Skewness	Point	Skewness of Point elevations, represents the skew of point distribution as a function of elevation	Elevated: 1-4 Near Surface: 0-1	Garcia et al., 2011 Hermosilla et al., 2014 Ediriweera et al., 2014 González-Ferreiro et al., 2014 Kramer et al., 2014
Variance	Point/ Intensity	Variation of elevation within fuel strata	Elevated: 1-4 Near Surface: 0-1	(Kramer et al., 2014)
Height Bins	Point	Number of points within height bin, divided by all points within the cell	Elevated: 1-1.5, 1.5-2, 2-2.5, 2.5-3, 3-3.5, 3.5-4, 1-4 Near Surface: 0-0.5, 0.5-1, 0-1	Garcia et al., 2011 Koetz et al., 2008 Popescu and Zhao, 2008 Erdody and Moskal, 2010 Heritage and Large, 2009 Mutlu et al., 2008 Skowronski et al., 2007 Skowronski et al., 2016 Kramer et al., 2014 Ediriweera et al., 2014 Hermosilla et al., 2014

3.2.4 Data Fusion

To investigate the effect of data fusion on the estimation of understory fuel hazard, image stacking and Principle Component Analysis (PCA) was used. Image stacking is a fusion technique where image bands or other derived raster datasets are combined into a single dataset. Image Stacking represents the simplest case of data fusion, the combination of multiple datasets (Mutlu et al., 2008). Principle Component Analysis (PCA) is a statistical fusion technique that is used to produce uncorrelated output bands, segregate noise components, and reduce the dimensionality of datasets (Jensen, 2005; Mutlu et al., 2008; Haywood et al., 2010).

The Composite Bands tool in ArcGIS (ESRI, 2011) was used to derive image stacks for each LiDAR metric type (points and intensity), a combination of both LiDAR metric types, and for each of these stacks including the standardised ADS40 imagery bands (See Table 3.2.3). The image stacks with both LiDAR metrics and ADS40 imagery were then statistically fused using PCA. From the uncorrelated PCA output bands, those greater than or equal to the first cumulative 95% of the variance in the data was used (see Table 3.2.3). The image stacks were then grouped by the data fusion method used (see Table 3.2.3).

Table 3.2.3: LiDAR metrics and image bands as well as a summary of Principle Component Analysis band details included in each image stack, grouped by data fusion method.

Fusion Method	Image Stack	LiDAR Metrics/Imagery		
Control	ADS40	ADS40 R G B		
	LiDAR Points	LiDAR Point Metrics		
	LiDAR Intensity	LiDAR Intensity Metrics		
	LiDAR Combined	LiDAR Point & Intensity Metrics		
Data Type	ADS40 + LiDAR Points	ADS40 R G B, LiDAR Point Metrics		
	ADS40 + LiDAR Intensity	ADS40 R G B, LiDAR Intensity Metrics		
	ADS40 + LiDAR Combined	ADS40 R G B, LiDAR Point & Intensity Metrics		
Statistical	PCA Band Characteristics	No. of PCA Components Taken	Cumulative Variance	Total No. of PCA Components
	ADS40 PCA	2	97.13%	3
	ADS40 + LiDAR Points PCA	8	95%	15
	ADS40 + LiDAR Intensity PCA	4	97%	7
	ADS40 + LiDAR Combined PCA	11	96.6%	19

3.2.5 Machine Learning

For this study, both a parametric, Maximum Likelihood Classification (MLC), and non-parametric Support Vector Machine (SVM) algorithm was chosen. Maximum likelihood classification is a commonly applied supervised image classification algorithm which utilises probability density functions to assign classes to pixels in unseen data. Pixels that are classified based on the highest probability a pixel falls into that class, determined from the distribution of classes in the input training dataset (Mustapha et al., 2010). A SVM is an ML algorithm which seeks to determine the optimal separating hyperplane between classes (Jensen, 2016). The data points, or vectors, that are closest to the hyperplane are used to delineate the classes; hence they are termed 'support vectors' (Pal and Mather, 2005). To control the robustness of the separating hyperplane, a trade-off between the location of the plane and misclassification error is controlled by a user defined constant, Cost (Pal and Mather, 2005). SVM's can be extended for non-linear decision boundaries (where classes are not linearly separable) by projecting data into a higher dimensional feature space through the use of a kernel function (Pal and Mather, 2005). For this study, a radial basis kernel was used, as it allowed for the investigation of a non-linear classification algorithm while keeping the number of parameters to be optimised to a minimum. Use of this kernel introduces only one other hyper-parameter relative to other kernels (Hsu et al., 2010) which controls the width of the Gaussian kernel (Foody et al., 2006).

Determination of the requisite SVM hyper-parameter values was done using a two layer grid search optimised against overall classification accuracy as recommended by Hsu et al. (2010). The first layer consisted of an order of magnitude search (9 orders), while the second layer involved a coarse grid search, ranged half an order of magnitude either side of the optimal values determined in the first layer. The resultant hyper-parameter values of this optimisation procedure are outlined in Table 3.2.4.

Table 3.2.4: Summary of optimised Supoort Vector Machine hyper-parameter values, computed using a two layer order of magnitude, and coarse search method.

| Investigation | Imagery | Elevated | | | | | | Near Surface | | | | | |
| | | Order of Magnitude Search | | | Coarse Search | | | Order of Magnitude Search | | | Coarse Search | | |
		Cost	Sigma	Overall Accuracy	Cost	Sigma	Overall Accuracy	Ccst	Sigma	Overall Accuracy	Cost	Sigma	Overall Accuracy
Control	ADS40	1E+02	1E-01	29.07%	7E+01	1E-01	29.17%	1E+05	1E-01	28.26%	6E+04	2E-01	28.42%
	LiDAR Points	1E-01	1E-01	34.48%	4E-01	3E-01	34.98%	1E+06	1E-04	28.16%	5E+05	7E-03	28.62%
	LiDAR Intensity	1E+03	1E-01	31.78%	7E+02	1E-01	31.84%	1E+02	1E-01	30.33%	5E+01	1E-01	30.45%
	LiDAR Combined	1E+05	1E-03	35.90%	3E+05	1E-03	36.48%	1E+06	1E-04	31.05%	4E+06	1E-04	31.41%
Data Type Fusion	ADS40 + LiDAR Points	1E+00	1E-01	36.23%	2E+00	5E-02	36.66%	1E+06	1E-03	30.92%	8E+05	8E-04	31.38%
	ADS40 + LiDAR Intensity	1E+05	1E-02	35.34%	8E+04	9E-03	35.79%	1E+02	1E-02	32.29%	1E+02	1E-02	32.29%
	ADS40 + LiDAR Combined	1E+00	1E-01	37.29%	5E+00	5E-02	37.52%	1E+00	1E-01	33.65%	5E-01	8E-02	33.83%
Statistical Fusion	ADS40 PCA	1E+00	1E+00	28.53%	6E-01	2E+00	28.73%	1E-01	1E+00	27.04%	8E-02	1E+00	27.22%
	ADS40 + LiDAR Points PCA	1E+00	1E-01	35.79%	9E-01	1E-01	35.95%	1E+01	1E-01	29.68%	8E+00	9E-02	30.33%
	ADS40 + LiDAR Intensity PCA	1E+01	1E-01	33.82%	4E+01	8E-02	34.16%	1E+02	1E-01	32.51%	5E+02	7E-02	32.54%
	ADS40 + LiDAR Combined PCA	1E+00	1E-01	37.82%	5E+00	7E-02	38.41%	1E+01	1E-01	34.54%	5E+00	9E-02	35.23%

3.2.6 Analysis

Classifier training and validation assessment was undertaken using the 'superclass()' function from the RStoolbox package based in the R statistical computing language (R Development Core Team, 2008; Leutner and Horning, 2016). This function takes an image and spatial polygons as input datasets and allows for the number of samples and method of validation to be specified; for this analysis 1000 samples per polygon and 5-fold cross validation were used, respectively. The training and validation dataset utilised in this analysis were derived by taking a 70% training, 30% validation random split stratified across fuel classes of the field data site polygons (see Section 3.2.2), using the Sample Design Tool (Buja, 2015) within ArcGIS (ESRI, 2011). A summary of the process used to derive the data products for this analysis provided in Appendix 3.

The validity and accuracy of the models developed in this analysis was determined using overall classification accuracy (OA), and the coefficient of agreement, Kappa (K) (Jensen, 2016); both of which are output by the 'superclass()' function used to train and validate the models. Overall classification accuracy represents the number of correctly classified pixels (for all classes, the diagonal of the confusion matrix), divided by all pixels that have been classified (Jensen, 2016). Overall classification accuracy does not however include an assessment of the errors of omission and commission within a confusion matrix. As such, K, which incorporates an assessment of the chance of agreement (the errors of omission and commission as represented by the column and row totals within a confusion matrix), is also computed (Jensen, 2016).

Another method for determining the accuracy/validity of classification models is to assess their accuracy on a per class basis. This was done in a similar manner to the calculation of OA. However per class accuracies are computed on a per row, or per column basis; termed User and Producer accuracies, respectively. User accuracy, computed across rows, indicates the probability that a pixel classified on a map actually represents the category on the ground and is a measure of commission (Jensen, 2016). Producer accuracy, computed down columns, indicates the probability of a reference pixel being correctly classified and is a measure of omission (Jensen, 2016). For this analysis, an accurate method for all categories is desirable. As such, User and Producer accuracies are used to investigate whether models are classifying better for certain classes than others, and the effect this has on the OA.

The results of this analysis are presented in three stages; the first two based on methods used to assess the the validity of the models, Overall Accuracy and User-Producer Accuracy. The Overall Accuracy section investigates both the potential to use LiDAR point and intensity metrics for understory fuel hazard estimation and compares the effects of data fusion methods. The third stage addresses the broader aim of this study to investigate the use of LiDAR, very high resolution imagery, data fusion and machine learning techniques to estimate understory fuel hazard in a wildland area. Within each of these, the the accuracy of different machine learning algorithms for the estimation of understory fuel hazard are also compared.

3.3 Results

3.3.1 Overall Accuracy

Overall accuracy results within this study were very low, <40% OA and 0.25 K, see Figure 3.3.1. However, when datasets from the different methods were compared, a number of general trends were exhibited. As the dimensionality (number of layers) between the Control and Data Type image stacks (see Table 3.2.3) increases , model performance improved. It was evident that across fuel hazard strata, the model performance increases with height; mean model performance for Elevated fuel strata was greater than that for Near Surface fuel strata. Performance of PCA models in Statistical Fusion, is of much greater variability than either the control or data type methods. In addition, the distribution of OA and K results for all methods, across both fuel strata are similar, as shown in Figure 3.3.1. When compared however, the values of K are lower, approximately half those of OA suggesting that the results of the models are not too distant from the null hypothesis, that the confusion matrices produced by the classifications are no better than random chance.

Control

Of all the methods the results of the Control method are the lowest. It can be seen in Figure 3.3.1 that both types of LiDAR metrics (point and intensity) derived for this analysis outperform the high resolution ADS40 imagery. This result is to be expected as the imagery product is unable to penetrate the canopy and measure understory vegetation structure used to estimate understory fuel hazard. When compared between the types, each metric type performs differently for the different fuel hazard strata modelled. Overall classification accuracy and K are greater for LiDAR point than LiDAR intensity metrics for Near Surface fuels, while the opposite relationship exists for Elevated fuels. When these metrics are used in combination it can be seen that the classification accuracy increases compared to the use of either metric type individually. There also exists a relationship between fuel strata and model performance variability. Results for Near Surface fuels exhibit small variability, while the results for Elevated fuels have relatively greater variability.

Data Type

When ADS40 imagery is introduced to the datasets modelled in the data type method, a slight improvement in model performance was seen. This suggests that combining multiple datatypes can improve model performance. However, as the imagery used for this method is not temporally consistent with the field data and LiDAR metrics used, the magnitude of this inference cannot be determined. The same relationships between LiDAR metric type, model variability and fuel strata were also exhibited.

Statistical Fusion

Statistical fusion produces the best performing model, ADS40 + LiDAR Combined PCA (SVM Elevated: 38.4 OA%, Near Surface: 35.2 OA%; MLC Elevated 33.0 OA%, Near Surface 29.7 OA%). However it can not be said that this method of fusion increases the accuracy of all models relative to those in the Data Type method. Instead, the spread of model performance is increased, reducing the ability to make inferences regarding the general effect of statistical
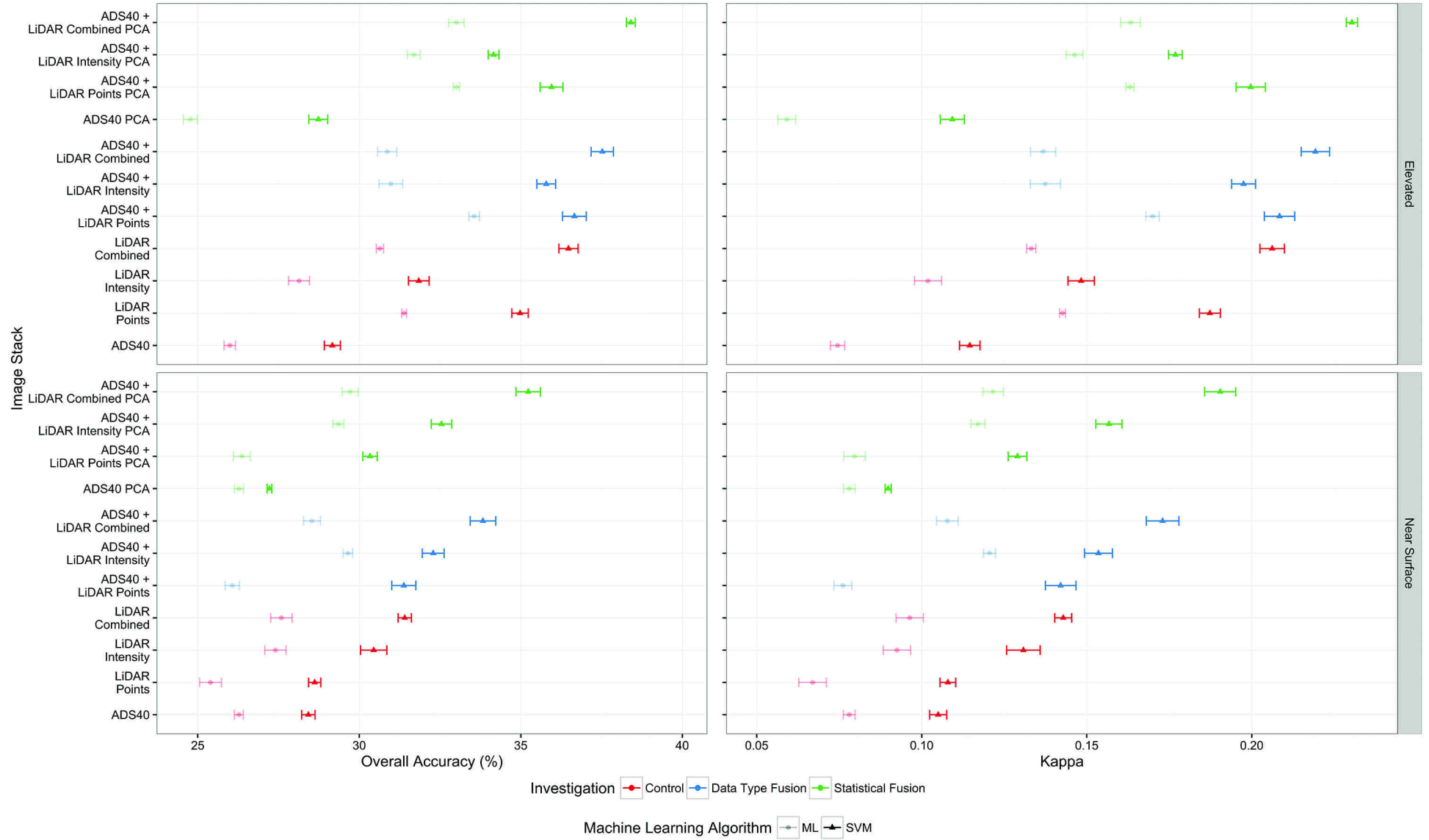
Figure 3.3.1: Overall Accuracy method organised by validation assessment metric (Overall Accuracy %, and Kappa) and understory fuel strata with 95% confidence intervals.

fusion for this analysis. It was also evident that the improvement introduced by statistical fusion is small (SVM Elevated: +0.9 OA%, Near Surface: +1.4 OA%; MLC Elevated: +2.1 OA%, Near Surface: +1.2 OA%) when compared to the next best performing model, ADS40 + LiDAR Combined.

3.3.2 User-Producer Accuracy

User and Producer accuracies for each fuel hazard class are illustrated in Figure 3.3.2. From this figure, a number of trends are exhibited. Comparing the shape of the User and Producer accuracy distributions it can be seen that although lower, the User accuracy is much more consistent per class than the Producer accuracy. This suggests that the models under investigation are more consistently making errors of commission than omission per class. However the inconsistency of the Producer accuracies both for individual and across classes infers that these results are no more reliable than those of the User accuracies.

3.3.3 Understory Fuel Hazard Classification Maps

Fuel hazard classification maps of the best performing models within each method (Control, Data Fusion, and Statistical Fusion) for each understory fuel strata are illustrated in Figure 3.3.3. It can be seen in these maps that Very High to Extreme Fuel hazard ratings correspond with the location of the heathlands (see Figure 3.2.1) in the eastern coastal side of the RNP and Low to Moderate fuel hazard ratings correspond in location with wet and dry sclerophyll forest in the inland western side of the RNP. Low fuel hazard ratings are also observed surrounding urbanised areas such as Bundeena and Heathcote (see Figure 3.3.3), which may be attributed to either the implementation of fuel management, or due to this being an common entry point for fires to enter the park through anthropogenic ignition.
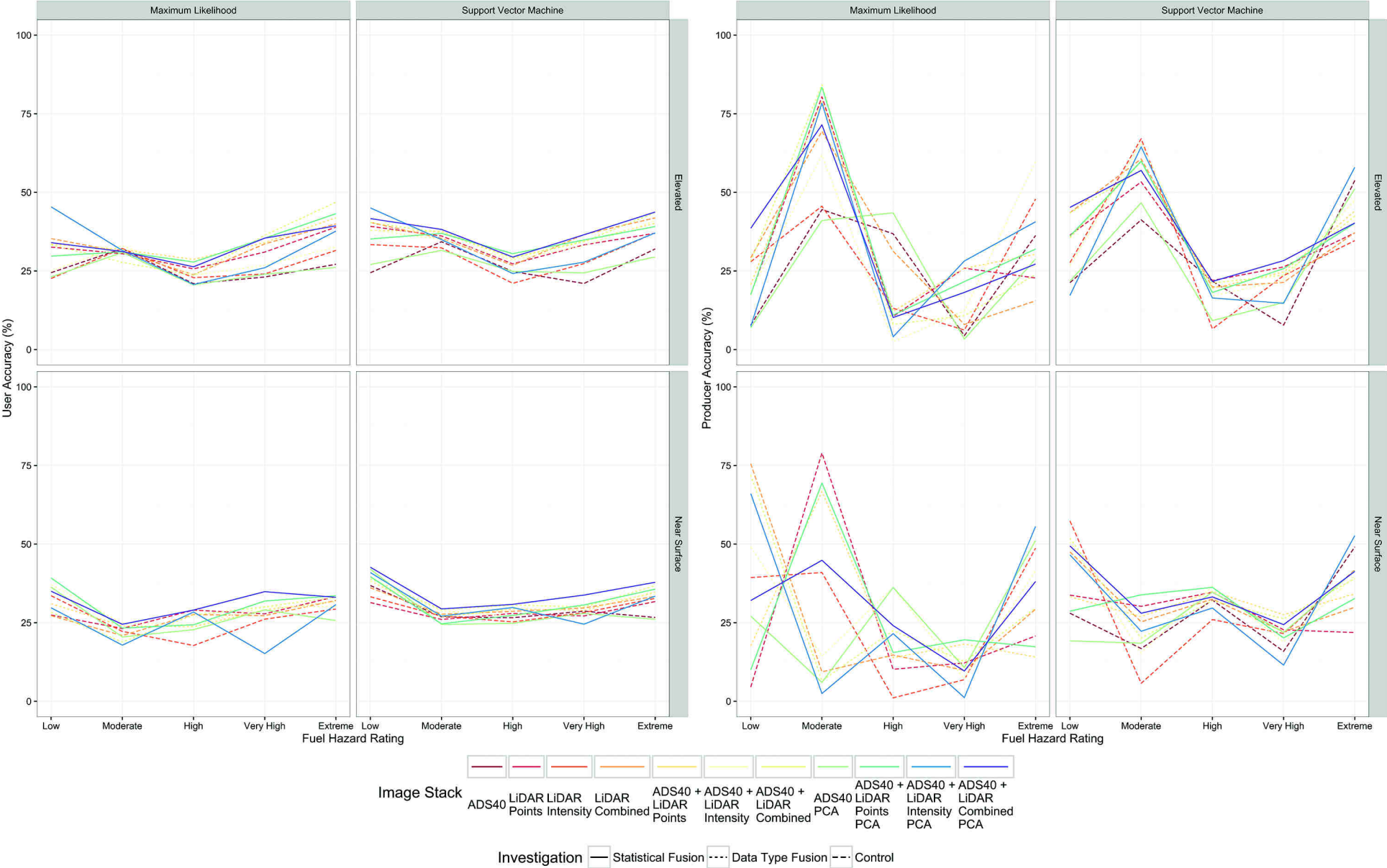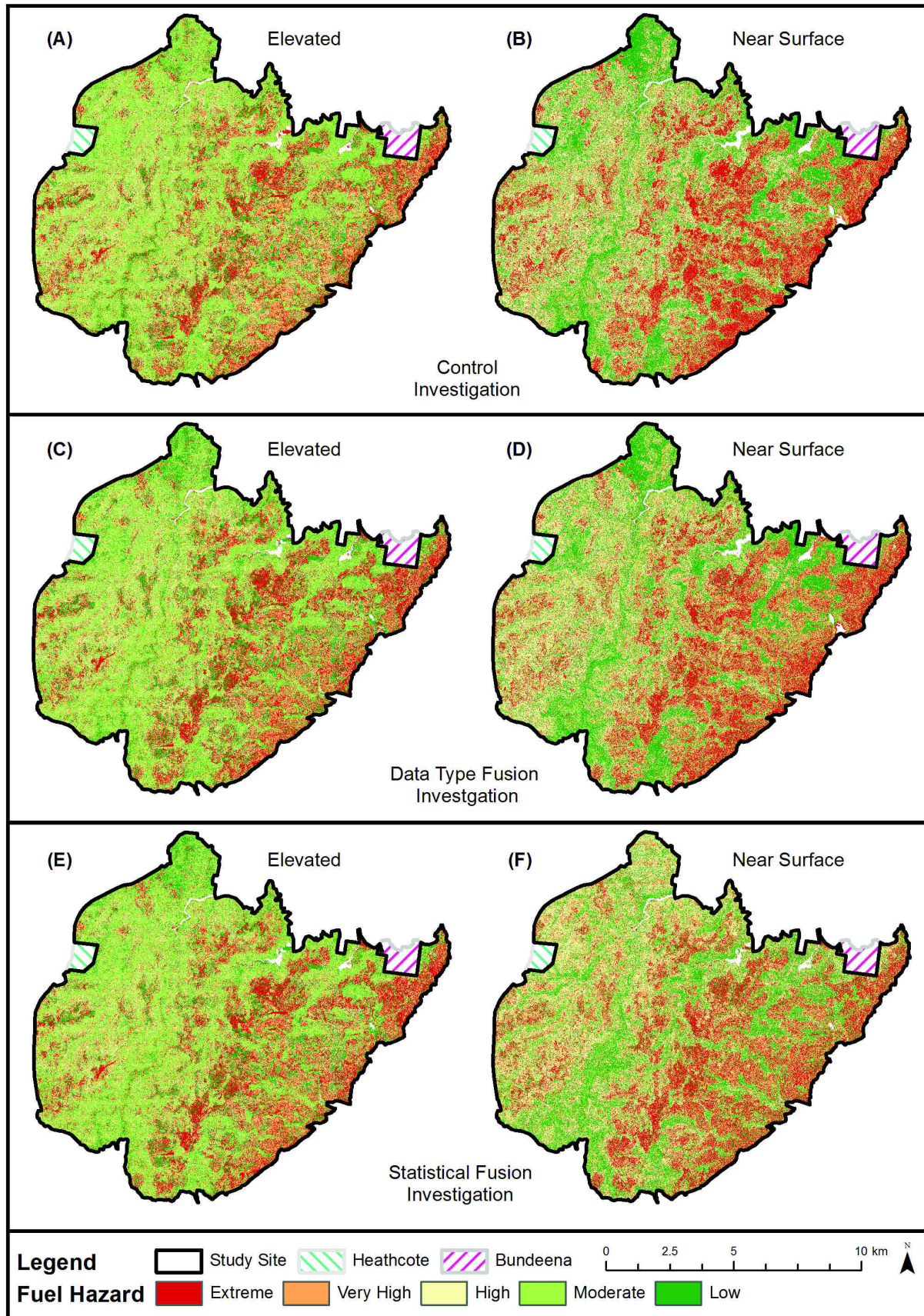
Figure 3.3.2: User-Producer method organised by understory fuel strata, and ML method.

Figure 3.3.3: Maps of the best performing fuel hazard classifications (A and B: LiDAR Combined. C and D: ADS40 + LiDAR Combined, E and F: ADS40 + LiDAR Combined PCA) for each method (Top: Control. Middle: Data Type. Bottom: Statistical), organised by understory fuel strata (Left: Elevated, Right: Near Surface).

3.4 Discussion

The results of this study indicate that the combined use of LiDAR point and intensity metrics, high resolution imagery and data fusion techniques are able to estimate the distribution of understory fuel hazard with low to moderate accuracy.

Currently there is only limited literature concerning the application of LiDAR to estimate fuel characteristics within Australia. The most analogous study Haywood et al. (2010), investigated the ability of LiDAR to estimate retrospective overall fuel hazard within the Victorian Central Highlands. Haywood et al. (2010), using LiDAR height bins and skewness metrics, PCA data fusion and MLC were able to produce overall fuel hazard estimates with moderate accuracy (48.72% OA LiDAR-Landsat stack, 56.41% OA PCA derived stack). Comparison with Haywood et al. (2010) infers that the results of this study, although objectively low in terms of more general image classification methods, are reasonable in terms of the estimation of fuel characteristics from LiDAR derived metrics for Australian vegetation.

A number of issues including the LiDAR metric derivation process, LiDAR sensor characteristics and vegetation effects, dataset temporal discrepancy and field data sampling method are thought to contribute to the low model performance in this study. As the complexity of overstory structure and amount of cover increases, the probability that LiDAR pulses are able to penetrate below the canopy is significantly decreased (Ediriweera et al., 2014). The reduction of LiDAR point density as a function of overstory cover results in low understory point density limiting the ability to derive metrics which accurately describe understory fuel structure. The magnitude of LiDAR pulse penetration is also affected by the relative size difference between the gaps in the canopy and the Instantaneous Field of View (IFOV) of the LiDAR sensor. This difference is determined by the altitude at which the sensor is flown (Goodwin, 2006). At the height at which LiDAR sensros are flown the difference between the sensor IFOV and gaps in the canopy is low reducing LiDAR pulse penetration of the canopy. These effects are compound to reduce the understory point density such that within some cells, the values of the LiDAR metrics can not be computed, producing missing values. For the method developed, smoothing, which takes the 3x3 focal mean of the surrounding cells, is used to fill these missing values. This procedure, while robust in its utilisation of local data points may not accurately represent the nature of understory vegetation within the filled areas. Resulting in training and validation data which confounds classification.

For LiDAR analyses of structures close to ground level (Near Surface fuel hazard) a common procedure is to set a minimum height boundary for example 50 cm (Goodwin, 2006) to filter out ground classified points. For this analysis, to have a sufficient point density for the computation of the LiDAR metrics a minimum height boundary has not been defined. By not setting this boundary, ground classified points may be introducing unnecessary noise into the metrics and reducing their ability to accurately represent the structure of fuels.
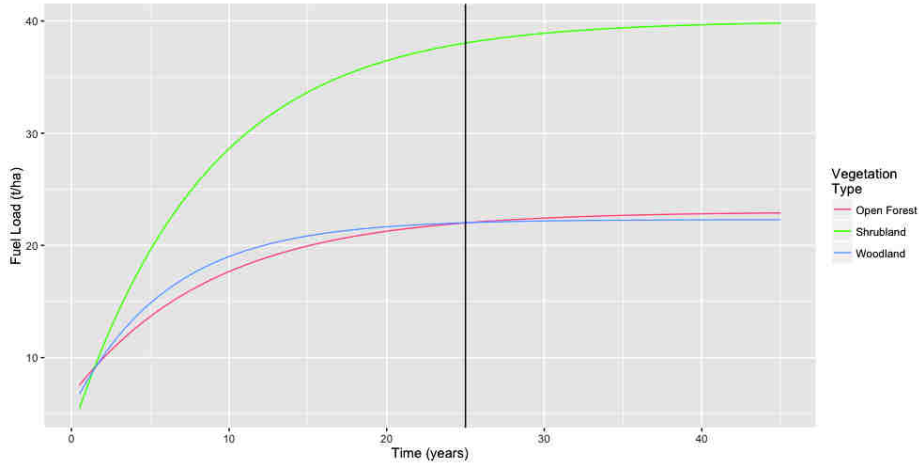
Figure 3.4.1: Conroy fuel load model [$F = a - c \cdot (e^{-bt})$, where a, b, c are constants for each vegetation type, t is time since last fire, and F is fuel load in tonnes/hectare] for various vegetation types (analogous to fuel vegetation groups, Conroy 1993). A black line indicates 25 years of fuel accumulation, the point at which accumulation rates have stabilised.

The temporal discrepancy of the input datasets is another issue which may have affected the ability of using multiple datasets to estimate understory fuel hazard. The ADS40 spectral signature, LiDAR structural measurements and field sampled fuel hazard measurements are a function of number of aspects of vegetation which should correspond when these sensors are used at the same, or within a short space of time. When data are not from the same date, a number of environmental processes may interact with vegetation on varying, and sometimes unquantifiable, timescales changing both its spectral signature and structure such that fuel hazard estimates derived between datasets may not correspond. An example of such an environmental process is fire itself which consumes fuel. Empirical models such as Conroy's fuel load model for the Sydney region, show that fuel accumulates for different vegetation types with the negative exponent of time (see Figure 3.4.1). This means that to accurately use datasets which are not temporally concurrent, they need to be recorded past 25 years after a fire, as this is the point at which fuel accumulation rates have stabilised. For this analysis we could not access temporally concurrent or datasets over this threshold. Haywood et al. (2010) also used input datasets from different dates, as such, the degree to which this affects the ability to estimate fuel hazard is unknown and for this analysis cannot be quantified.

To reduce the time taken to collect data points for this analysis, multiple assessors were used. When fuels which exhibit arrangements or structural aspects for which the visual estimation methodology does not have a description, an assessor has to subjectively assign a fuel hazard rating. Watson et al. (2012) determined that this subjectivity can lead to significant variation in the assessment of fuels of the same arrangement. In their study, variation between assessors resulted from differing perceptions of the extent to which plot characteristics fitted, as well as alignment observed vegetation arrangements to the fuel hazard level descriptions. Within this study, assessor subjectivity is hypothesised to introduce a significant loss in accuracy due to the low number of calibration assessments undertaken (one away from the study site, and one for each time assessors went into the field), and the assessors relative inexperience in the

assessment of fuels.

Field sites were located with a standard GPS receiver, accurate to 10 m. This was undertaken due to financial, time and portability constraints of more accurate handheld, or differential GPS devices respectively. When compared to similar literature (Haywood et al., 2010)which utilise LiDAR metrics for the estimation of vegetation structures, this method is seen to be less valid, as these studies use a more significantly accurate position to correctly register their input datasets. Within the method developed, it is intended that this source of error be minimised by incorporating the GPS inaccuracy into the fuel hazard site buffer. This was undertaken with independent consideration of the processing resolution used for this analysis. When considered together, it can be seen that incorporating the GPS inaccuracy in this way the location and assessment accuracy actually decrease. Error is introduced in this way due to the misclassification of pixels included within the buffer. That may, or may exhibit the fuel hazard rating recorded for that area. In a similar manner the assessment radius also acts as a source of error. The value for this radius was taken from the OFHAG as the value for which fuel is assessed. However in the field, the area produced by a radius of this distance was not defined or visualised by the assessors. As such the assessment radius may not be consistent between assessors, nor between sites. It can also be seen that bias may be introduced, due to the height difference (~165 cm and ~197 cm, respectively) between assessors and their height relative to that of the surrounding vegetation (~0.5 m - +2 m).

From the literature concerning the assessment of fuel hazard, there is little guidance regarding the type of sampling design method which should be employed (Watson, 2009). At most, either an unspecified number of point samples should be taken evenly spaced across an area and averaged (Watson, 2009), or that 10 samples should be taken along a 'sample walk' and averaged to estimate fuel hazard for a 20 ha area (Gould, 2007). Initially, the latter of these methods was to be employed for this analysis. However, due to the time constraints this method could not be implemented. The validity of the area assessed by this method could also not be reconciled by the author, where the height and topography of the vegetation would act to obscure visual estimation, were taken into consideration. The initial method settled on, was to take an average fuel hazard rating of paired sample sites along the paths accessed. However, it was identified that within these pairs fuel structures could be varied substantially, greater then up or down a single hazard rating as suggested by the OFHAG (Hines et al., 2010). Constraints such as time, weather, and spatial coverage also impacted on field sampling, which resulted in the decision to drop the paired nature of this method. It is hypothesised that error is introduced where non-overlapping, but spatially clustered sample sites are included for training/validation. Clustered sites are thought to bias both the spatial accuracy, and diversity of fuel hazard rating measurements within the dataset.

3.5   Conclusion

Within this study, fusing imagery with LiDAR metrics which utilise both intensity and elevation measurements provided the most accurate results. This demonstrates that the data fusion of LiDAR and ADS40 Imagery can be used to estimate understory fuel hazard in a wildland area. The model developed can be used to produce understory fuel hazard rating maps for land management agencies to plan and implement fuel management practices. The high resolution of these maps enables their use with fire behaviour simulation models, which could enable more realistic and accurate predictions of fire spread and intensity.

3.5.1 Future Work

Future work should investigate the combination of point elevation and intensity metrics for the assessment of understory vegetation structure. In addition, a standardised method to normalise and atmospherically correct LiDAR intensity measurements should be developed. This would enable increased use of LiDAR intensity data. Drone based LiDAR is suggested as a method to improve the robustness of the LiDAR point cloud, therefore improving derived metric quality. Drones can be used alongside a number of optical remote sensors as well as LiDAR, and provide a number of benefits including low material and operational costs, flexible spatial and temporal resolution, and high-intensity data collection (Tang and Shao, 2015). Critically, drones are able to fly at significantly lower altitudes than those permitted for full sized aircraft. A lower flight altitude would correspondingly reduce the LiDAR sensor IFOV increasing the relative allowing greater canopy penetration, for a more precise measurement of understory vegetation structure (see Section 3.4).

3.6   Acknowledgements

3.7   References

See combined reference list at the end of the thesis.

Chapter 4 Conclusion

4.1 Synthesis of key findings

Within Australia, there is currently a limited body of research concerning the use of RS to assess fuel characteristics. This thesis investigates the ability of RS to measure fuel hazard (which accounts for the arrangement of fuels in a complex (Hines et al., 2010)) at higher spatial resolutions, and determine whether RS can measure fuel hazard in multiple fuel strata. Studies in this thesis are located in the Royal National Park NSW Australia, where there have been no recent significant fire events, allowing fuel recovery and accumulation .

Chapter 2 addresses Aim 1, investigating the ability of high resolution imagery from different dates to assess fuel hazard and integrating pan-sharpening to arbitrarily determine image resolution. Independent of resolution, no single effect that could be attributed to pan-sharpening was identified. In fitting linear models to Overall Accuracy OA% vs image resolution plots. Pan-sharpened imagery exhibited low slope values ($<$1 OA% vs m-resolution) and variable slope directions, indicating the plausible use of pan-sharpening as a method to improve the resolution of fuel hazard classification. A per fuel hazard class analysis identified that High and, Very High and Extreme fuel hazard ratings were most consistently classified with accuracy $>$10% for User and Producer accuracies, respectively.

Chapter 3 addresses Aim 2, to use LiDAR, high resolution imagery, data fusion and machine learning classification techniques to estimate understory fuel hazard within a wildland area. Point elevation and intensity LiDAR metrics were determined to most accurately classify Elevated fuel hazard when combined with ADS40 imagery, statistically fused using principal component analysis, and classified with a Support Vector Machine (SVM) (38.4 OA%, 0.23 Kappa (K)). Statistical fusion resulted in the best performing models for SVM classification and similar results for data type fusion for Maximum Likelihood Classification (MLC), when examined across understory fuel strata. However, within the SVM classification results, use of data type fusion was more consistent than statistical fusion when compared to the results of the control method. For both OA% and K, SVM classification outperformed MLC across both understory fuel strata and data fusion methods.

The implications of this thesis are that it is possible to use a high resolution imagery fused with that from different dates, and LiDAR metrics for fuel hazard classification. The results suggest that future research to improve fuel hazard classification should utilise data fused from a range of RS instruments, and classified with non-parametric machine learning algorithms.

4.2 Directions for future work

Future avenues of research arising from the findings of this research include:

1. The use RS datasets, both high resolution imagery and LiDAR, obtained using drones. Drones are able to capture data at much lower altitudes than permitted for aircraft, over similar spatial extents at a significantly lower cost (Tang and Shao, 2015). A lower cost enables the capture of more temporally frequent high resolution images, while lower altitudes permit greater LiDAR pulse penetration through the canopy measuring understory fuel structure in greater detail.

2. The use of a mobile handheld LiDAR scanner, such as Zebedee (Bosse et al., 2012), to supplement the subjective visual estimation of fuel hazard in the field. This scanner has been shown that it is possible to automatically derive information for different understory vegetation components from a ground-based LiDAR point cloud (Marselis et al., 2016). Use of such a scanner would enable precise point based characterisation of understory fuel structures. Which could then be correlated with point clouds captured using airborne LiDAR scanners for precision fuel hazard estimation over large spatial extents.

References

Amarsaikhan, D., Saandar, M., Ganzorig, M., Blotevogel, H. H., Egshiglen, E., Gantuyal, R., Nergui, B. and Enkhjargal, D. (2012), 'Comparison of multisource image fusion methods and land cover classification', *International Journal of Remote Sensing* **33**(8), 2532–2550.

Andersen, H.-E., McGaughey, R. J. and Reutebuch, S. E. (2005), 'Estimating forest canopy fuel parameters using LIDAR data', *Remote Sensing of Environment* **94**(4), 441–449.
URL: *http://linkinghub.elsevier.com/retrieve/pii/S0034425704003438*

Arroyo, L. A., Pascual, C. and Manzanera, J. A. (2008), 'Fire models and methods to map fuel types: The role of remote sensing', *Forest Ecology and Management* **256**(6), 1239–1252.
URL: *http://www.sciencedirect.com/science/article/pii/S0378112708005410*

Baltsavias, E. P. (1999), 'Airborne laser scanning: basic relations and formulas', *ISPRS Journal of Photogrammetry and Remote Sensing* **54**(2), 199–214.

Birth, G. S. and McVey, G. R. (1968), 'Measuring the color of growing turf with a reflectance spectrophotometer', *Agronomy Journal* **60**(6), 640–643.

Bosse, M., Zlot, R. and Flick, P. (2012), 'Zebedee: Design of a spring-mounted 3-d range sensor with application to mobile mapping', *IEEE Transactions on Robotics* **28**(5), 1104–1119.

Bowman, D. M. J. S., Balch, J. K., Artaxo, P., Bond, W. J., Carlson, J. M., Cochrane, M. A., D'Antonio, C. M., DeFries, R. S., Doyle, J. C. and Harrison, S. P. (2009), 'Fire in the Earth system', *Science* **324**(5926), 481–484.

Brandis, K. and Jacobson, C. R. (2003), 'Estimation of vegetative fuel loads using Landsat TM imagery in New South Wales, Australia', *International Journal of Wildland Fire* **12**(2), 185–194.

Buja, K. (2015), 'Sampling Design Tool'.
URL: *http://www.arcgis.com/home/item.html?id=ecbe1fc44f35465f9dea42ef9b63e785*

Caccamo, G., Chisholm, L. A., Bradstock, R. A., Puotinen, M. L. and Pippen, B. G. (2012), 'Monitoring live fuel moisture content of heathland, shrubland and sclerophyll forest in south-eastern Australia using MODIS data', *International Journal of Wildland Fire* **21**(3), 257–269.

Cash, A. (2012), Assessing the capabilities of Landsat imagery for measuring fuel properties in Sydney Coastal Dry Sclerophyll Forest, PhD thesis, School of Earth & Environmental Science, University of Wollongong.
URL: *ttp://ro.uow.edu.au/thsci/34*

Catchpole, W. R. and Wheeler, C. J. (1992), 'Estimating plant biomass: a review of techniques', *Australian Journal of Ecology* **17**(2), 121–131.

Chafer, C. J., Noonan, M. and Macnaught, E. (2004), 'The post-fire measurement of fire severity and intensity in the Christmas 2001 Sydney wildfires', *International Journal of Wildland Fire* **13**(2), 227–240.

Cheney, N. P. (1994), 'The effectiveness of fuel reduction burning for fire management', *Fire and Biodiversity: the Effects and Effectiveness of Fire Management* (8), 7–16.

Cheney, N. P. and Sullivan, A. L. (2008), *Grassfires: fuel, weather and fire behaviour*, CSIRO, Canberra, Australia.

Chuvieco, E. and Kasischke, E. S. (2007), 'Remote sensing information for fire management and fire effects assessment', *Journal of Geophysical Research: Biogeosciences* **112**(G1).

Conroy, B. (1993), 'Fuel management strategies for the Sydney region', *The Burning Question: Fire Management in NSW'.(Ed. J Ross) pp* pp. 73–83.

Countryman, C. M. (1969), Fuel evaluation for fire control and fire use, *in* 'Symposium on fire ecology and control and use of fire in wildland management, Tucson, AZ'.

Cruz, M. G. and Gould, J. S. (2009), Field-based fire behaviour research: past and future roles, *in* 'Proceedings of the 18th World IMACS Congress and MODSIM09 International Congress on Modelling and Simulation 13-17 July', Citeseer, pp. 247–253.

Cruz, M. G., Gould, J. S., Alexander, M. E., Sullivan, A. L., McCaw, W. L. and Matthews, S. (2015), *A guide to rate of fire spread models for Australian vegetation*, East Melbourne, Victoria Australasian Fire and Emergency Service Authorities Council Ltd and Commonwealth Scientific and Industrial Research Organisation.

Cruz, M. G., Sullivan, A. L., Leonard, R., Malkin, S., Matthews, S., Gould, J. S., McCaw, W. L. and Alexander, M. E. (2014), Fire Behaviour Knowledge in Australia spread prediction capability and application, Technical Report June, Bushfire Cooperative Research Centre, East Melbourne, Victoria.

Davies, G. M., Hamilton, A., Smith, A. M. S. and Legg, C. J. (2008), 'Using visual obstruction to estimate heathland fuel load and structure', *International Journal of Wildland Fire* **17**(3), 380.

Ediriweera, S., Pathirana, S., Danaher, T. and Nichols, D. (2014), 'LiDAR remote sensing of structural properties of subtropical rainforest and eucalypt forest in complex terrain in North-eastern Australia', *Journal of Tropical Forest Science* **23**(3), 397–408.

Environmental Systems Research Institute (2011), 'ArcGIS Desktop: Release 10.3'.
   URL: *https://www.arcgis.com*

Erdody, T. L. and Moskal, M. L. (2010), 'Fusion of LiDAR and imagery for estimating forest canopy fuels', *Remote Sensing of Environment* **114**(4), 725–737.
   URL: *http://linkinghub.elsevier.com/retrieve/pii/S0034425709003277*

Exelis Visual Information Solutions (2016*a*), 'ENVI 5.3'.
   URL:
   http://www.harrisgeospatial.com/ProductsandSolutions/GeospatialProducts/ENVI.aspx

Exelis Visual Information Solutions (2016*b*), 'IDL 8.5'.
   URL:
   http://www.harrisgeospatial.com/ProductsandSolutions/GeospatialProducts/IDL.aspx

Ferster, C. J. and Coops, N. C. (2014), 'Assessing the quality of forest fuel loading data collected using public participation methods and smartphones'.
   URL: *http://dx.doi.org/10.1071/WF13173*

Finney, M. A. and Andrews, P. L. (1999), 'FARSITE - a program for fire growth simulation', *Fire Management Notes* **59**(2), 13–15.

Fogarty, L. G., Pearce, G., Catchpole, W. R. and Alexander, M. E. (1998), Adoption vs. adaptation: lessons from applying the Canadian forest fire danger rating system in New Zealand, *in* 'Proceedings, 3rd International Conference on Forest Fire Research and 14th Fire and Forest Meteorology Conference, Luso, Coimbra, Portugal', pp. 1011–1028.

Foody, G. M., Mathur, A., Sanchez-Hernandez, C. and Boyd, D. S. (2006), 'Training set size requirements for the classification of a specific class', *Remote Sensing of Environment* **104**(1), 1–14.

Frolking, S., Palace, M. W., Clark, D. B., Chambers, J. Q., Shugart, H. H. and Hurtt, G. C. (2009), 'Forest disturbance and recovery: A general review in the context of spaceborne remote sensing of impacts on aboveground biomass and canopy structure', *Journal of Geophysical Research: Biogeosciences* **114**(G2).

Garcia, M., Riaño, D., Chuvieco, E., Salas, J. and Danson, F. M. (2011), 'Multispectral and LiDAR data fusion for fuel type mapping using Support Vector Machine and decision rules', *Remote Sensing of Environment* **115**(6), 1369–1379.

Geoscience Australia (2015), 'Digital Elevation Model (DEM) of Australia derived from LiDAR 5 Metre Grid'.
URL: *http://dx.doi.org/10.4225/25/5652419862E23*

Ghassemian, H. (2016), 'A review of remote sensing image fusion methods', *Information Fusion* **32**, 75–89.

González-Ferreiro, E., Diéguez-Aranda, U., Crecente-Campo, F., Barreiro-Fernández, L., Miranda, D. and Castedo-Dorado, F. (2014), 'Modelling canopy fuel variables for Pinus radiata D. Don in NW Spain with low-density LiDAR data', *International Journal of Wildland Fire* **23**(3), 350.

Goodwin, N. R. (2006), 'Assessing understorey structural characteristics in eucalypt forests: an investigation of LiDAR techniques'.
URL: *http://handle.unsw.edu.au/1959.4/28365*

Gorrod, E. J. and Keith, D. A. (2009), 'Observer variation in field assessments of vegetation condition: implications for biodiversity conservation', *Ecological Management & Restoration* **10**(1), 31–40.

Gould, J. S. (2007), *Field guide: fuel assessment and fire behaviour prediction in dry eucalypt forest*, CSIRO.

Gould, J. S. and Cruz, M. G. (2012), Australian Fuel Classification: Stage II. Ecosystem Sciences and Climate Adaption Flagship, Technical report, Ecosystem Sciences and Climate Adaption Flagship, Canberra, Australia.

Gould, J. S., McCaw, W. L., Cheney, N. P., Ellis, P. F., Knight, I. K. and Sullivan, A. L. (2008), *Project Vesta: fire in dry eucalypt forest: fuel structure, fuel dynamics and fire behaviour*, CSIRO Publishing.

GRASS Development Team (2016), 'Geographic Resources Analysis Support System (GRASS GIS) Software: Release 7.3'.
URL: *http://grass.osgeo.org*

Haywood, A., Mellor, A. and Siggens, A. (2010), Fuel Hazard Mapping of the Victorian Central Highlands Using Lidar Data., *in* '15th Australian Remote Sensing & Photogrammetry Conference, Alice Springs Northern Territory, Australia, 13 - 17 September 2010.'.

Heritage, G. and Large, A. (2009), *Laser scanning for the environmental sciences*, John Wiley & Sons.

Hermosilla, T., Ruiz, L. A., Kazakova, A. N., Coops, N. C. and Moskal, M. L. (2014), 'Estimation of forest structure and canopy fuel parameters from small-footprint full-waveform LiDAR data', *International Journal of Wildland Fire* **23**(2), 224–233.

Hexagon Geospatial (2015), 'ERDAS Imagine 2015'.
URL: *http://www.hexagongeospatial.com/products/producer-suite/erdas-imagine*

Hines, F., Tolhurst, K. G., Wilson, A. A. G. and McCarthy, G. J. (2010), Overall fuel hazard assessment guide, Technical Report 82.
URL:
http://www.fireandbiodiversity.org.au/_literature_173786/Overall_fuel_hazard_assessment_guide_4t

Hollis, J. J., Gould, J. S., Cruz, M. G. and Doherty, M. D. (2011), 'Scope and Framework for an Australian Fuel Classification. A Report for the Australasian Fire and Emergency Service Authorities Council'.

Hollis, J. J., Gould, J. S., Cruz, M. G. and McCaw, W. L. (2015), 'Framework for an Australian fuel classification to support bushfire management', *Australian Forestry* **78**(1), 1–17.

Hsu, C.-W., Chang, C.-C. and Lin, C.-J. (2010), 'A practical guide to support vector classification'.
URL: *http://www.csie.ntu.edu.tw/ cjlin/papers/guide/guide.pdf*

Huete, A., Didan, K., Miura, T., Rodriguez, E. P., Gao, X. and Ferreira, L. G. (2002), 'Overview of the radiometric and biophysical performance of the MODIS vegetation indices', *Remote Sensing of Environment* **83**(1), 195–213.

Intergovernmental Committee on Surveying & Mapping (2010), 'ICSM LiDAR Acquisition Specifications and Tender Template'.
URL:
http://www.icsm.gov.au/elevation/LiDAR_Specifications_and_Tender_Template.pdf

Isenberg, M. (2016), 'LAStools - efficient tools for LiDAR processing'.
URL: *http://lastools.org*

Jacobson, C. R. (2010), 'Use of linguistic estimates and vegetation indices to assess post-fire vegetation regrowth in woodland areas', *International Journal of Wildland Fire* **19**(1), 94–103.

Jakubowksi, M. K., Guo, Q., Collins, B., Stephens, S. and Kelly, M. (2013), 'Predicting Surface Fuel Models and Fuel Metrics Using Lidar and CIR Imagery in a Dense, Mountainous Forest', *Photogrammetric Engineering and Remote Sensing* **79**(1), 37–49.

James, G. (2013), 'An introduction to statistical learning : with applications in R'.
URL: *http://dx.doi.org/10.1007/978-1-4614-7138-7*

Jawak, S. D. and Luis, A. J. (2013), 'A comprehensive evaluation of PAN-sharpening algorithms coupled with resampling methods for image synthesis of very high resolution remotely sensed satellite data', *Advances in Remote Sensing* **2013**.

Jensen, J. R. (2005), *Introductory digital image processing : a remote sensing perspective*, 3rd ed edn, Upper Saddle River, N.J. : Prentice Hall.

Jensen, J. R. (2016), *Introductory digital image processing : a remote sensing perspective*, 4th editio edn, Glenview, IL Pearson Education, Inc.

Jin, S. and Chen, S.-C. (2012), 'Application of QuickBird imagery in fuel load estimation in the Daxinganling region, China', *International Journal of Wildland Fire* **21**(5), 583.
  URL:
  http://www.publish.csiro.au/view/journals/dsp_journal_fulltext.cfm?nid=114&f=WF11018

Kane, V. R., North, M. P., Lutz, J. A., Churchill, D. J., Roberts, S. L., Smith, D. F., McGaughey, R. J., Kane, J. T. and Brooks, M. L. (2014), 'Assessing fire effects on forest spatial structure using a fusion of Landsat and airborne LiDAR data in Yosemite National Park', *Remote Sensing of Environment* **151**, 89–101.

Kaufman, Y. J. and Tanre, D. (1992), 'Atmospherically resistant vegetation index (ARVI) for EOS-MODIS', *IEEE transactions on Geoscience and Remote Sensing* **30**(2), 261–270.

Keane, R. E. (2015), *Wildland Fuel Fundamentals and Applications*, number 1, Springer International Publishing, Cham.
  URL: *http://link.springer.com/10.1007/978-3-319-09015-3*

Keane, R. E., Burgan, R. E. and van Wagtendonk, J. (2001), 'Mapping wildland fuels for fire management across multiple scales: Integrating remote sensing, GIS, and biophysical modeling', *International Journal of Wildland Fire* **10**(4), 301–319.
  URL: *http://www.publish.csiro.au/paper/WF01028*

Keith, D. A. (2004), *Ocean shores to desert dunes: the native vegetation of NSW and the ACT*, Department of Environment and Conservation (NSW).

Koetz, B., Morsdorf, F., der Linden, S., Curt, T. and Allgöwer, B. (2008), 'Multi-source land cover classification for forest fire management based on imaging spectrometry and LiDAR data', *Forest Ecology and Management* **256**(3), 263–271.

Kramer, H., Collins, B., Kelly, M. and Stephens, S. (2014), 'Quantifying Ladder Fuels: A New Approach Using LiDAR', *Forests* **5**(6), 1432–1453.
  URL: *http://www.mdpi.com/1999-4907/5/6/1432/htm*

Land & Property Information NSW (2008), 'Porthacking 50cm Orthorectified Imagery'.
  URL: *https://sdi.nsw.gov.au/sdi.nsw.gov.au/catalog/search/resource/details.page?uuid={6A6AA8F5-5A82-4752-97A3-B82B3D5B39E6}*

Land & Property Information NSW (2011), 'HawksburySOUTH L0049'.
  URL: *https://sdi.nsw.gov.au/sdi.nsw.gov.au/catalog/search/resource/details.page?uuid={1169CF31-043D-4211-8181-E9C8764A5EC0}*

Land & Property Information NSW (2013), 'The Native Vegetation of the Sydney Metropolitan Area VIS_ID 3817'.
  URL: *https://sdi.nsw.gov.au/catalog/search/resource/details.page?uuid=%7B2CCFE4F6-4743-4597-AAEA-8575A0DF12DA%7D*

Lary, D. J., Alavi, A. H., Gandomi, A. H. and Walker, A. L. (2016), 'Machine learning in geosciences and remote sensing', *Geoscience Frontiers* **7**(1), 3–10.
URL: *http://www.sciencedirect.com/science/article/pii/S1674987115000821*

Lefsky, M. A., Cohen, W. B., Acker, S. A., Parker, G. G., Spies, T. A. and Harding, D. (1999), 'Lidar remote sensing of the canopy structure and biophysical properties of Douglas-fir western hemlock forests', *Remote Sensing of Environment* **70**(3), 339–361.

Leutner, B. and Horning, N. (2016), *RStoolbox: Tools for Remote Sensing Data Analysis*.
URL: *https://cran.r-project.org/package=RStoolbox*

Marselis, S. M., Yebra, M., Jovanovic, T. and van Dijk, A. I. J. M. (2016), 'Deriving comprehensive forest structure information from mobile laser scanning observations using automated point cloud classification', *Environmental Modelling & Software* **82**, 142–151.

McArthur, A. G. (1958), The preparation and use of fire danger tables, *in* 'Proceedings of the Fire Weather Conference', Bureau of Meteorology, Melbourne, Australia.

McArthur, A. G. (1960), *Fire danger rating tables for annual grasslands*, Canberra, A.C.T. : Forestry and Timber Bureau.

McArthur, A. G. (1966*a*), 'Prescribed burning in Australian fire control', *Australian Forestry* **30**(1), 4–11.

McArthur, A. G. (1966*b*), *Weather and grassland fire behaviour*, Forestry and Timber Bureau, Department of National Development, Commonwealth of Australia.

McArthur, A. G. (1967), 'Fire behaviour in eucalypt forests'.

McCarthy, G. J., Tolhurst, K. G. and Chatto, K. (1999), *Overall fuel hazard guide*, Fire Management, Department of Natural Resources & Environment.

Merrill, D. F. and Alexander, M. E. (1987), 'Glossary of forest fire management terms'.

Middlemann, M. H. (2007), *Natural hazards in Australia : identifying risk analysis requirements*, Canberra : Geoscience Australia.
URL: *http://www.ga.gov.au/news/index.jsp#nathaz*

Moritz, M. A., Morais, M. E., Summerell, L. A., Carlson, J. M. and Doyle, J. C. (2005), 'Wildfires, complexity, and highly optimized tolerance.', *Proceedings of the National Academy of Sciences of the United States of America* **102**(50), 17912–7.
URL: *http://www.pnas.org.simsrad.net.ocs.mq.edu.au/content/102/50/17912.short*

Muir, J., Schmidt, M., Tindall, D., Trevithick, R., Scarth, P. and Stewart, J. B. (2011), Field measurement of fractional ground cover, Technical report, Queensland Department of Environment and Resource Management for the Australian Bureau of Agricultural and Resource Economics and Sciences, Canberra, Australia.

Mustapha, M. R., Lim, H. S. and Iafri, M. Z. M. (2010), 'Comparison of Neural Network and Maximum Likelihood Approaches in Image Classification', *Journal of Applied Sciences* **10**(22), 2847–2854.

Mutlu, M., Popescu, S. C., Stripling, C. and Spencer, T. (2008), 'Mapping surface fuel models using lidar and multispectral data fusion for fire behavior', *Remote Sensing of Environment* **112**, 274–285.

National Parks & Wildlife Service NSW (2000), 'Royal National Park, Heathcote National Park and Garawarra State Recreational Area: Plan of Management', (February).

Nordkvist, K., Granholm, A.-H., Holmgren, J., Olsson, H. and Nilsson, M. (2012), 'Combining optical satellite data and airborne laser scanner data for vegetation classification', *Remote Sensing Letters* **3**(5), 393–401.

Office of Environment & Heritage NSW (2016), 'NSW Fire History Geodatabase'.

Pal, M. and Mather, P. M. (2005), 'Support vector machines for classification in remote sensing', *International Journal of Remote Sensing* **26**(5), 1007–1011.

Popescu, S. C. and Zhao, K. (2008), 'A voxel-based lidar method for estimating crown base height for deciduous and pine trees', *Remote Sensing of Environment* **112**(3), 767–781.

R Development Core Team (2008), 'R: A Language and Environment for Statistical Computing: Version 3.3.1'.
URL: *http://www.r-project.org*

Roff, A., Goodwin, N. R. and Merton, R. (2005), Assessing fuel loads using remote sensing: Technical report summary, Technical report, New South Wales Rural Fire Service Technical Report, 2006, 42 (12): 63-67.

Rollins, M. G., Keane, R. E. and Parsons, R. A. (2004), 'Mapping fuels and fire regimes using remote sensing, ecosystem simulation, and gradient modeling', *Ecological Applications* **14**(1), 75–95.

Rouse Jr, J., Haas, R. H., Schell, J. A. and Deering, D. W. (1974), 'Monitoring vegetation systems in the Great Plains with ERTS', *NASA special publication* **351**, 309.

Skowronski, N. S., Clark, K. L., Nelson, R., Hom, J. and Patterson, M. (2007), 'Remotely sensed measurements of forest structure and fuel loads in the Pinelands of New Jersey', *Remote Sensing of Environment* **108**(2), 123–129.

Skowronski, N. S., Haag, S., Trimble, J., Clark, K. L., Gallagher, M. R. and Lathrop, R. G. (2016), 'Structure-level fuel load assessment in the wildland-urban interface: a fusion of airborne laser scanning and spectral remote-sensing methodologies'.
URL: *http://dx.doi.org/10.1071/WF14078*

Sullivan, A. L. (2009*a*), 'Wildland surface fire spread modelling, 1990 - 2007. 2: Empirical and quasi-empirical models', *International Journal of Wildland Fire* **18**(4), 369.
URL:
http://www.publish.csiro.au/view/journals/dsp_journal_fulltext.cfm?nid=114&f=WF06142

Sullivan, A. L. (2009*b*), 'Wildland surface fire spread modelling, 1990 - 2007. 3: Simulation and mathematical analogue models', *International Journal of Wildland Fire* **18**(4), 387.
URL:
http://www.publish.csiro.au/view/journals/dsp_journal_fulltext.cfm?nid=114&f=WF06144

Tang, L. and Shao, G. (2015), 'Drone remote sensing for forestry research and practices', *Journal of Forestry Research* **26**(4), 791–797.
URL: *"http://dx.doi.org/10.1007/s11676-015-0088-y*

Tolhurst, K. G., Shields, B. and Chong, D. M. (2008), 'Phoenix: Development and Application of a Bushfire Risk Management Tool', *The Australian Journal of Emergency Management* **23**(4), 47.

Turner, R. (2007), 'An overview of Airborne LiDAR applications in New South Wales state forests', *Australian and New Zealand Institute of Foresters* (June 2007), 1–22.
URL: *http://www.forestry.org.au/pdf/pdf-public/conference2007/papers/Turner Russell Lidar.pdf*

USGS (2016), 'Earth Explorer'.
URL: *http://earthexplorer.usgs.gov/*

Watson, P. J. (2009), 'Understanding bushfire fuels: A report for the NSW Rural Fire Service'.

Watson, P. J., Penman, S. H. and Bradstock, R. A. (2012), 'A comparison of bushfire fuel hazard assessors and assessment methods in dry sclerophyll forest near Sydney, Australia', *International Journal of Wildland Fire* **21**(6), 755–763.

Whelan, R. J., Kanowski, P., Gill, A. M. and Andersen, A. (2006), 'Living in a land of fire'.

Williams, R. J., Gill, A. M. and Bradstock, R. A. (2012), *Flammable Australia: Fire Regimes, Biodiversity and Ecosystems in a Changing World*, CSIRO.
URL: *https://books.google.com.au/books?id=DghUhpiiVCsC*

Zhang, J. (2010), 'Multi-source remote sensing data fusion: status and trends', *International Journal of Image and Data Fusion* **1**(1), 5–24.

Zhao, K., Popescu, S. C., Meng, X., Pang, Y. and Agca, M. (2011), 'Characterizing forest canopy structure with lidar composite metrics and machine learning', *Remote Sensing of Environment* **115**(8), 1978–1996.

Appendicies

4.3   Appendix 1

Plot of pixel values from NDVI images taken for each field data collection period. A strong goodness of fit ($R^2_{adj} = 0.94$) between NDVI images demonstrates low phenological variation between them.

$y = 0.0423 + 0.961\,x$

$R^2_{adj} = 0.94$
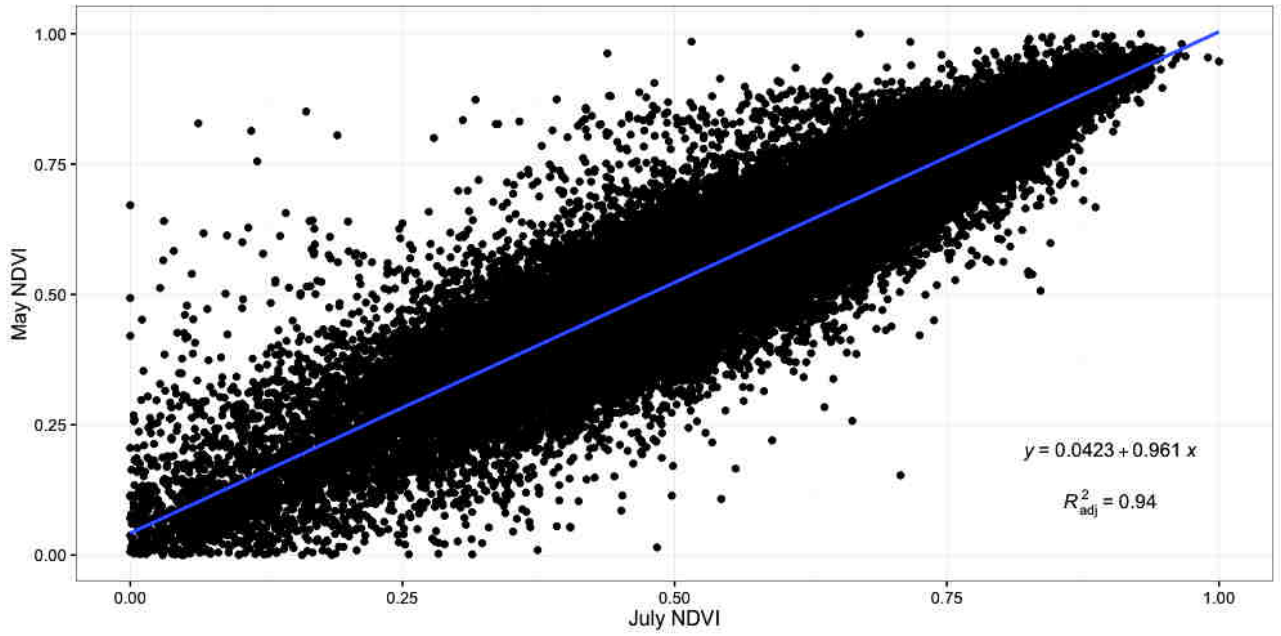
4.4 Appendix 2

Data flow diagram summarising the steps used to derived imagery for paper: Estimating fuel hazard using optical datasets from different dates with pan-sharpening.
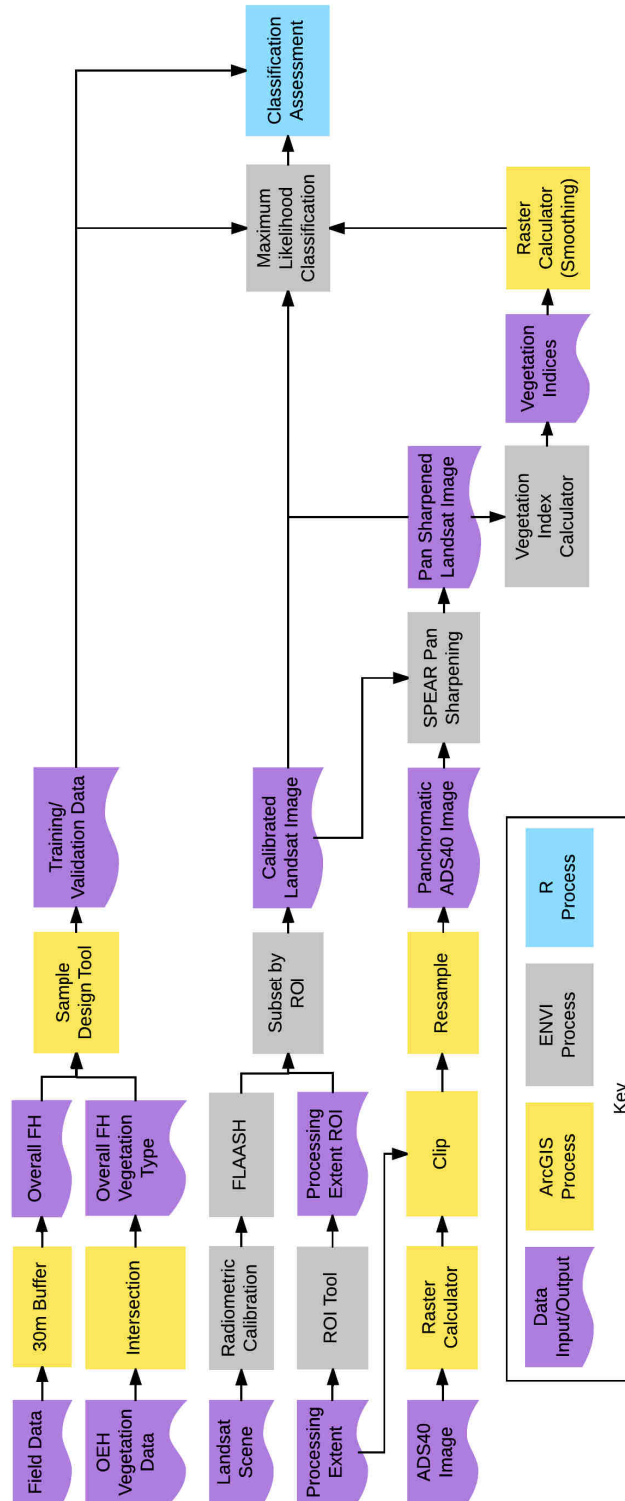
4.5   Appendix 3

Data flow diagram summarising the steps used to derived imagery for paper: Classifying understory fuel hazard using LiDAR and high resolution imagery, integrating fusion and machine learning